Flood hazard assessment for Mekong Delta

Appendix 6 to the Annex 1 to the
Stage 2 Evaluation Report

November 2009

Final Report

Contents

1 Introduction 1

2 Flood hazard assessment procedure 2

2.1 General 2

2.2 Determination of the flood hazard 2

3 Description of focal areas 3

3.1 General 3

3.2 Focal areas 5

3.3 Hydrological network and data availability 6

3.4 Hydrological characteristics 6

3.4.1 Rainfall 6

3.4.2 Evaporation 8

3.4.3 River flows 8

3.4.4 Tidal boundaries 9

4 Hydraulic model of the Delta 11

4.1 General 11

4.2 Model layout 11

4.3 Mekong at Kratie 13

4.4 Tributary inflow to Tonle Sap Lake 15

4.5 Tributary inflow to Mekong 16

4.6 Rainfall 16

4.7 Evaporation 17

4.8 Water use 17

4.9 Sea boundary 17

5 Flood hazard assessment 18

5.1 General 18

5.1.1 Description of scenarios 18

5.1.2 Outline 19

5.2 Probabilistic analysis 19

5.2.1 Annual maximum water levels 19

5.2.2 Maximum water levels in the early flood season 24

5.2.3 Fitted function 24

5.3 Resulting flood maps for the Base Case 25

5.4 Results for development scenarios [2]-[5] 26

5.4.1 Hydraulic model output 26

5.4.2 Estimating flood hazards from 11 simulated years 26

5.4.3 Results for scenario [2] – Cam0 28

5.4.4 Results for Scenario [3] – Vna 32

5.4.5 Results for Scenario [4] – Vnd 35
5.4.6 Results for Scenario [5] – Cam0Vna 38
5.5 Scenario [6] – flood diversion to the Tonle Sap lake 41
5.6 Sea level rise 45
6 Conclusions and recommendations 48
6.1 Conclusions 48
6.2 Recommendations 49
7 Literature 50

1 Introduction

In the Mekong Delta 4 Focal Areas have been selected by the CNMC and the VNMC concentrated along the border between Cambodia and Vietnam, including:

1. Takeo, west of Bassac in Cambodia
2. Prey Veng, east of Mekong in Cambodia
3. Long Xuyen Quadrangle, west of Bassac in Vietnam, and
4. Plain of Reeds, east of Mekong in Vietnam

Flood hazard assessment in these Focal Areas involves the determination of flood levels for distinct return period from 2 to 100 years with the duration and time of occurrence of the flood. The latter is particularly of importance in relation to the timing of harvest of the crop. For this purpose simulation runs with the ISIS-model of the delta, a one-dimensional hydraulic model, have been carried out, covering 97 years of historical floods from 1910 to 2006.

For the management of floods and related risks in the Focal Areas in the Mekong Delta the following development scenarios have been considered:

- Scenario_0: Existing condition of land use and flood control levels in Cambodia and Vietnam;
- Scenario_1: Vietnamese Focal Areas provided with complete flood control and Cambodian Focal Areas unchanged;
- Scenario_2: Cambodian Focal Areas provided with early flood control and Vietnamese Focal Areas unchanged;
- Scenario_3: Vietnamese Focal Areas provided with full flood control, Cambodian Focal Areas provided with early flood control, and
- Scenario_4: Diversion to the Tonle Sap for early flood control.

The set up of this Appendix 6 is as follows. In Chapter 2 the flood hazard assessment procedure for the Mekong Delta floods is presented followed by a description of the Focal Areas and hydrological characteristics of the Mekong Delta in Chapter 3. The hydraulic model of the Mekong delta is presented in Chapter 4 with the applied boundary conditions. In Chapter 5 the flood hazard in the Mekong Delta is discussed for the above mentioned scenarios, whereas in Chapter 6 the effect of sea level rise on the water levels in the Mekong and Bassac is estimated. Finally, in Chapter 7 conclusions and recommendations are made.

Reference is made to Appendix 7 to 11 to Annex 1 of the Stage 1 Report for details of the applied hydraulic model (Appendix 7), applied boundary conditions in the hydraulic model (Appendix 8 and 9), probabilistic computations (Appendix 10) and modelling of the flow diversion to Tonle Sap (Appendix 11). These appendices give a detailed description of the data used and procedures applied.

2 Flood hazard assessment procedure

2.1 General

The floods in the Mekong Delta are classified as a special type of flood in the Lower Mekong Basin due to their special external and internal boundary conditions and the delta's unique hydraulic infrastructure. The flood levels in the Mekong Delta in its downstream part are essentially the result of upstream and lateral inflow, local rainfall and downstream water levels at sea. The flood in the Mekong delta is conveyed via the Mekong and Bassac Rivers and via their flood plains, including the colmatage canal system which diverts and controls the flow from and to the River. In the delta the river regime is modified by to the temporary storage in Tonle Sap Lake and in the Mekong flood plains, creating slowly rising and falling water levels.

2.2 Determination of the flood hazard

For the Mekong delta downstream of Kratie for flood hazard assessment use is made of the fact that a relatively long historical discharge series at Stung Treng just upstream of Kratie is available. Furthermore, for the tributary inflow further downstream and to the Tonle Sap Lake long representative series have been created preserving the serial and cross-correlation with the Mekong flow. The series, which cover the period 1910-2006, are used as boundary conditions for a hydrodynamic model (based on ISIS-modelling package) to derive a 97-year series of water levels in the flood-prone areas. Further input to the model is formed by local rainfall, evaporation, water use and the year 2000 tidal conditions at the Gulf of Thailand and the South China Sea.

The relevant statistics including the probabilities of flooding and related damages for return periods from 2 to 100 years can be derived directly from the series of water levels and depths computed with the model. From the model results for each year maximum water levels and flood damages are derived for all model nodes to estimate the exceedance probabilities. The probability estimates are obtained with Gringortens formula:

$$p_i = \frac{r_i - 0.44}{N + 0.12} \qquad (2.1)$$

where:

p_i = probability of exceedance of the annual maximum water level in year *i*
N = total number of years
r_i = rank number of the maximum water in year *i* (1 = highest, n = lowest)

Since the series of annual maxima is close to 100 years, the estimated 100-year water level is by definition approximately the same as the maximum observed water level.

3 Description of focal areas

3.1 General

The Mekong Delta comprises the BDP-Sub-areas 9 and 10, see Figure 3.1 and Figure 3.2, and covers the Mekong river basin from Kratie to the river mouth in the South China Sea. The total area amounts about 144,500 km^2 of which 105,100 km^2 is in Cambodia, 4,200 km^2 in Thailand and 35,200 km^2, the Cuu Long Delta, is located in the southern part of Vietnam. A number of river reaches can be distinguished:

1. From Kratie via Kampong Cham to Chroy Changvar (Phnom Penh), just upstream where the Tonle Sap River joins the Mekong and the Bassac branches off at Chaktomouk Junction to discharge part of the total Mekong flow to the sea;
2. The Tonle Sap River and Lake with its large number of tributaries covering a drainage area of nearly 86,000 km^2.
3. Mekong from Phnom Penh to the North Vam Nao River junction, with discharge stations Neak Luong in Cambodia and Tan Chau in Vietnam. The North Vam Nao River diverts part of the Mekong flow to the Bassac;
4. Mekong downstream of North Vam Nao River, discharging its water to the South China Sea via a number of branches: Co Chien, Ham Luong, Cua Dai, and Cua Tieu. The total Mekong flow is measured in this reach at My Thuan;
5. Bassac from Chaktomouk Junction to the junction with North Vam Nao River, with stream gauging stations Chaktomouk in Cambodia and Chau Doc in Vietnam. Downstream of Chaktomouk the basin of the Prek Thnot discharges to the Bassac;
6. Bassac downstream of the junction with North Vam Nao River to the South China Sea with the flow measured at Can Tho. Part of the flow from the right bank of the Bassac drains via the Cai Lon River to the Gulf of Thailand.

The Tonle Sap Lake, the flood plains and the road infrastructure play an important role in storing and conveying the floodwaters.

Apart from the fringes of the basins of the Tonle Sap and the Prek Thnot basin the areas is very flat. In general, the delta has a deep hollow shape: high along the riverbanks and low toward the inland. Regarding land use, the area around Tonle Sap is predominantly covered with forest of which a small part is flooded forest forming an important habitat for fish reproduction and refuge. Here some 25% of the land cover is agricultural land. The land use in the delta is heavily dominated by paddy land, with some forest in the upper parts. Soils in the delta are the most fertile of the LMB, brought in by the floods. Large quantities of gleysols exist suitable for rice farming. In the lower part of the delta intrusion of saline water affects the quality of the soils. Infertile acid sulphate soils are found in the Plain of Reeds.

Reference is made to Annex 1 of Volume 2 of the Inception Report for a full description of the characteristics of the Mekong Delta included in the Sub-Areas 9 and 10.

Figure 3.1 Layout of Tonle Sap River and Lake basin

Figure 3.2 Layout of Mekong Delta in Sub-Area 10, comprising the Focal Areas

3.2 Focal areas

In the Mekong Delta 4 Focal Areas have been selected by the CNMC and the VNMC concentrated along the border between Cambodia and Vietnam, including:

1. Takeo, west of Bassac in Cambodia
2. Prey Veng, east of Mekong in Cambodia

3. Long Xuyen Quadrangle, west of Bassac in Vietnam, and
4. Plain of Reeds, east of Mekong in Vietnam

The location of the Focal Areas in the Mekong Delta is as follows:

1. Focal Area Takeo is located in Takeo and Kandal Provinces west of the Bassac, enclosed by the right bank of the Bassac , Road Nr 2 from Takmau to the Cambodian-Vietnamese border.
2. Focal Area Prey Veng is located in Prey Veng Province between the left bank of the Mekong, Road Nr 1, border of the Prey Veng and Svay Rieng Provinces and the Cambodian-Vietnamese border.
3. Long Xuyen Quadrangle boundaries are formed by the right bank of Bassac River from Chau Doc to Kenh Cai San off-take of Bassac d/s of Long Xuyen, the Cambodian-Vietnamese border from Chau Doc to Ha Tien, the Rach Gia-Ha Tien Canal from Hat Tien to Rach Soi via Kien Luong, Hon Dat and Rach Gia and the Kenh Cai San from Rach Soi to the Bassac via Tan Hiep. Most of this area is located in the An Giang and Kien giang Provinces and a small part in Hau Giang Province
4. The Plain of Reeds is bordered by the left bank of the Mekong from Hong Ngu near Tan Chau to Thanh Binh, in the south by the Nguyen Van Tiep canal via My An to My Phuoc, the Tong Doc Loc, crossing the West Vaico, Thu Thua canal, west of Road 1A from My Tho to Ben Luc via Tan An, the Bo Bo canal parallel to the East Vaico river in the west and in the north by the Cambodian-Vietnamese border up to the Mekong River at Hong Ngu. The area is in the provinces Dong Thap, Long An and Tien Giang.

3.3 Hydrological network and data availability

The Mekong Delta encloses the BDP-Sub-areas 9 and 10. The hydro-meteorological monitoring network and data availability has been described in detail in Annex 1 to Volume 2 of the Inception Report to which reference is made.

3.4 Hydrological characteristics

3.4.1 Rainfall

The Mekong delta has a monsoon climate. The average annual rainfall varies from 1,200 to 2,000 mm and around Tonle Sap from 1,300 to 1,600 mm. The seasonal distribution of the rainfall for Kampong Cham, Battambang and Tra Cu in Vietnam is shown in respectively Figure 3.3 to Figure 3.5. The rainfall is seen to be distributed into two seasons:

- the dry season from November to April receives some 10% of the annual rainfall, while
- the rainy season from May to November receives the remaining 90%.

From the graphs it is observed that - different from the upper part of the Mekong basin - in the delta also October is a wet month.

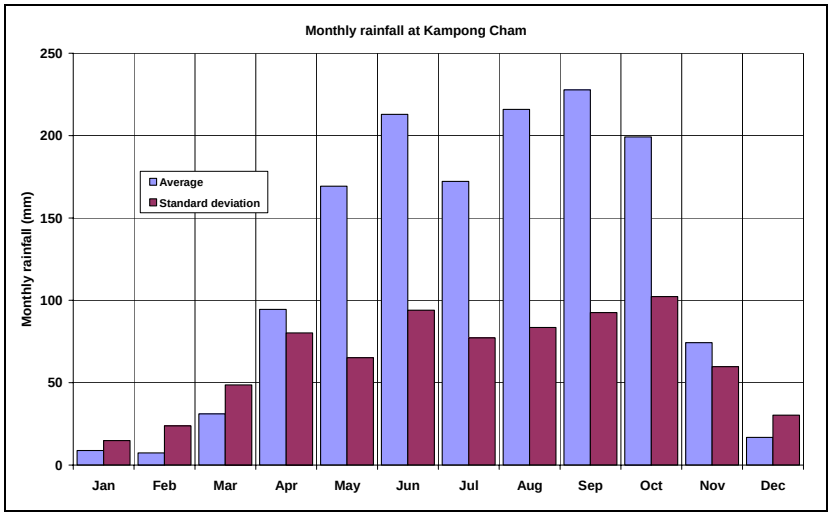

Figure 3.3 Monthly rainfall characteristics of Kampong Cham (Cambodia)

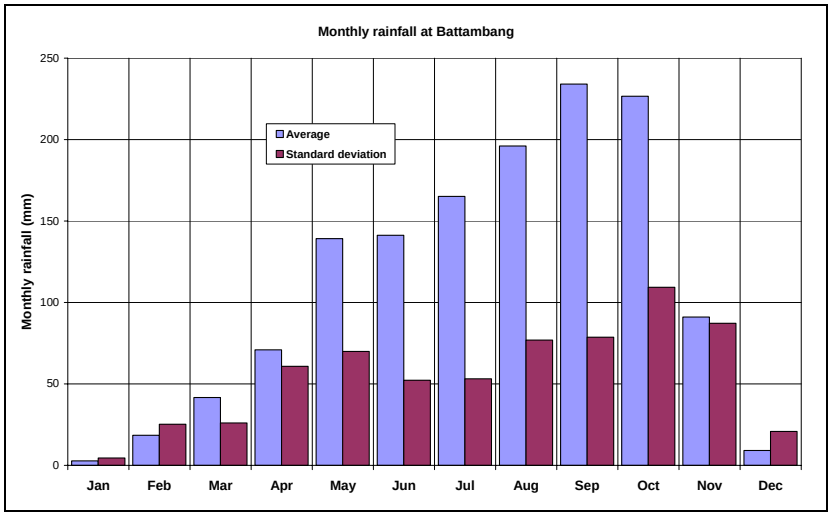

Figure 3.4 Monthly rainfall characteristics of Battambang (Cambodia)

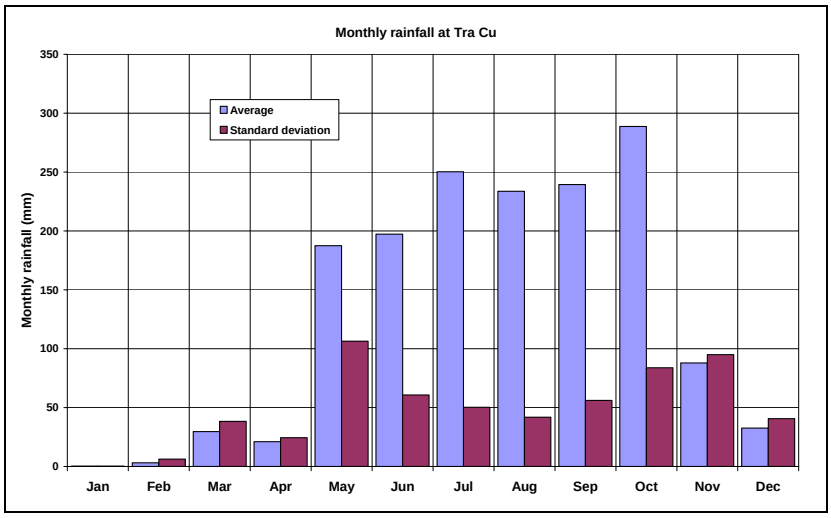

Figure 3.5 Monthly rainfall characteristics of Tra Cu (Vietnam)

3.4.2 Evaporation

Annual (pan)-evaporation in the Mekong basin in Cambodia varies between 1300 and 1900 mm. For the Mekong Delta in Vietnam annual total between 900 and 1300 mm are reported. Monthly pan-evaporation data generally are highest in the March-April and lowest in July-September/October.

3.4.3 River flows

Upstream inflows

The inflow to the delta is to a large extent determined by the discharge in the Mekong at Kratie. In Phase 1 an analysis has been made of the water level record and discharge measurements at Kratie and of the stations Pakse and Stung Treng. Since the discharge at Stung Treng is apart from a time shift of one day approximately equal to the flow at Kratie and because this series was considered to be more reliable and available for a longer period it was taken as the inflow to the Mekong Delta instead of the series of Kratie. Reference is made to Appendix 8 for the details.

The monthly flow statistics of the Mekong at Stung Treng for the Period 1910-2006 is presented in Table 3.1 and Figure 3.6. Largest flows are observed in the months August and September and lowest in March-April.

Table 3.1 Monthly flow statistics (MCM) of the Mekong at Stung Treng, Period 1910-2006

Var	Jan	Feb	Mar	Apr	May	Jun	Jul	Aug	Sep	Oct	Nov	Dec	Year
mean	10,879	7,315	6,114	5,573	10,131	28,918	61,130	99,625	100,254	61,855	29,066	16,622	437,480
stdev	1,779	1,155	1,097	1,368	3,407	11,029	16,277	21,651	18,043	14,036	6,564	3,186	60,258
cv	0.164	0.158	0.179	0.245	0.336	0.381	0.266	0.217	0.180	0.227	0.226	0.192	0.138
min	7,205	4,780	3,426	1,931	3,391	9,922	26,355	52,390	51,462	31,474	16,788	9,945	285,292
max	15,596	9,740	8,957	9,329	23,141	67,019	102,090	160,875	147,218	101,193	46,386	23,618	553,923

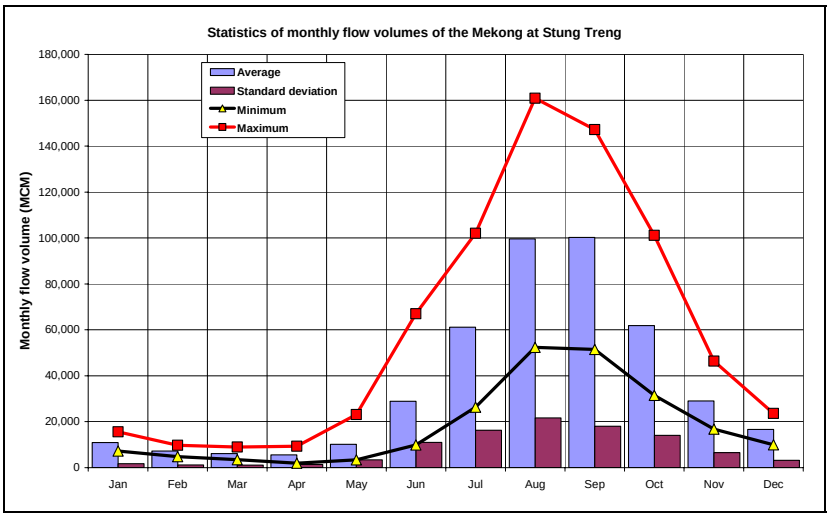

Figure 3.6 Monthly flow statistics of the Mekong at Stung Treng, Period 1910-2006

Lateral inflow

Downstream of Kratie the inflow to the Mekong is from the 13 Stungs draining to the Tonle Sap Lake and the Mekong tributaries Prek Te, Prek Chhlong, Prek Thnot. Their monthly averages are presented in Table 3.2.

Table 3.2 Average monthly tributary inflow (in MCM) to the Tonle Sap lake (observations of years 1997-2004) and to the Mekong downstream of Kratie (SWAT series 1985-2006)

	Jan	Feb	Mar	Apr	May	Jun	Jul	Aug	Sep	Oct	Nov	Dec	Year
Tonle Sap	487	271	271	312	783	1,616	2,783	4,740	5,581	6,638	2,947	926	27,354
Prek Te	114	60	34	27	42	87	160	369	633	587	358	201	2,671
P. Chhlong	84	44	32	26	43	79	84	163	278	340	228	133	1,533
P. Thnot	77	58	40	88	192	236	337	395	505	675	299	153	3,054

The statistics of the tributary inflow to the Tonle Sap are shown also in Figure 3.7. It is observed that on average the inflow is largest in October, in response to the rainfall, see Figure 3.4, In comparison with the Mekong, as shown in Figure 3.6, it follows that the inflow regime to the Tonle Sap is shifted by about one month. This gives excellent opportunities to use the Tonle Sap Lake for temporary storage of the early flood of the Mekong to reshape the regime downstream of Phnom Penh for harvesting in late August. On the other hand, during the year 2000, when the flood volume of the Mekong was large, the inflow to Tonle Sap Lake from its tributaries was also large. The annual inflows to the Tonle Sap are correlated with the flow volume in the Mekong upstream of the Delta; more than half of the variance on the inflow is explained by the Mekong flow volume.

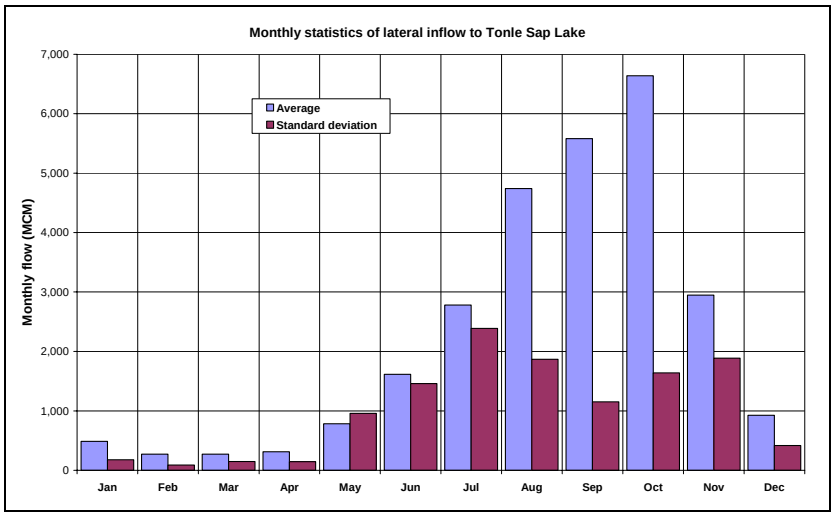

Figure 3.7 Average and standard deviation of monthly inflows to Tonle Sap Lake, Period 1997-2004

3.4.4 Tidal boundaries

The downstream boundary of the Mekong Delta is formed by the Gulf of Thailand in the west and the South China Sea in the south:

- The tide in the Gulf of Thailand varies from semi-diurnal to diurnal. The tidal range is in the order of 1.5 m. Levels are highest in October and November.

- In the South China Sea the tide is basically semi-diurnal, but becomes at times almost diurnal. The daily range is generally in the order of 1.5 to 2.5m; the maximum range is about 4 m, see Figure 3.8. The tidal averages show a sharp increase in September-October coinciding with highest flows in the Mekong as shown for 4 coastal stations in Figure 3.9.

The annual maximum water levels of station Tra Vinh near the coast, which is available from 1985 till 2006 does not show clear effects of wind set up in the mouth of the Mekong. The annual maximum values during the available 22 years only varied from 1.58 to 1.82 masl.

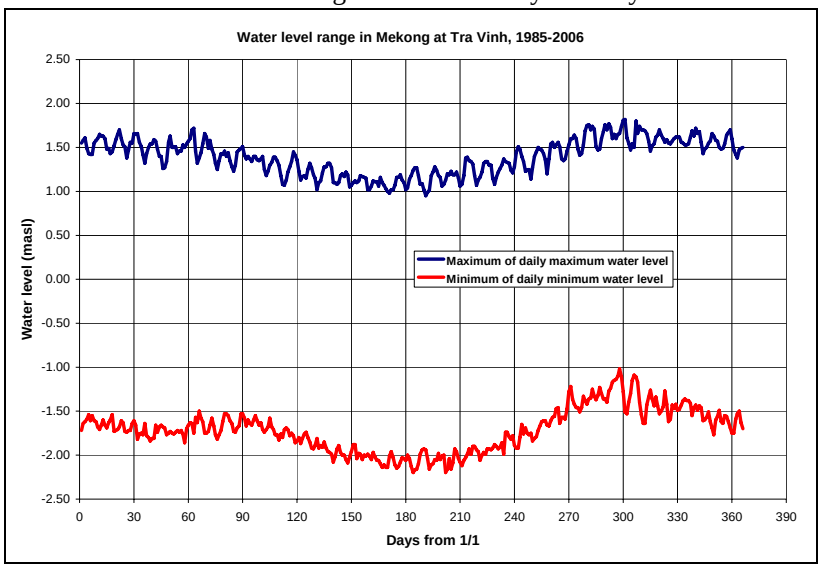

Figure 3.8 Water level range in Mekong at Tra Vinh near the coast, Period 1985-2006

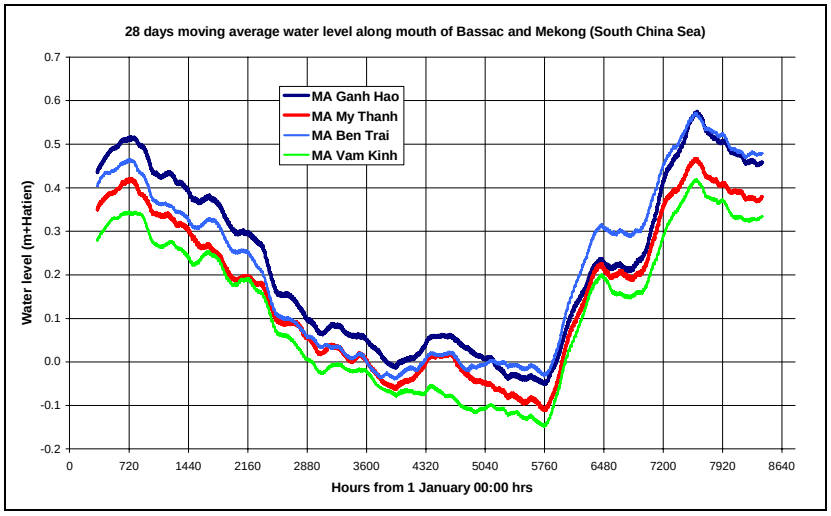

Figure 3.9 28 days moving average of water level at Ganh Hao, My Thanh, Ben Trai and Vam Kinh

4 Hydraulic model of the Delta

4.1 General

In this chapter an overview is given of the hydraulic model of the Mekong Delta and its boundary conditions as for flood hazard assessment. The model is used to compute flood levels for distinct return period from 2 to 100 years with the duration and time of occurrence of the flood, based on 97 years of historical floods from 1910 to 2006. First the model layout is shortly discussed and subsequently the boundary conditions, including:

- upstream boundary condition at Kratie,
- tributary inflow to Tonle Sap Lake,
- tributary inflow to Mekong,
- rainfall,
- evaporation,
- water use, and
- downstream boundary condition at Gulf of Thailand and South China Sea.

4.2 Model layout

The hydraulic model of the Mekong Delta is based on the ISIS modelling system for the simulation of unsteady flow in channel networks. It provides an implicit numerical solver for the de Saint Venant equations for 1 dimensional flow. At selected intervals it computes water levels and discharges on a non-staggered grid. The system was introduced to the MRC under the WUP-A programme and now serves as part of the Decision Support Framework (DSF). The model covers the Mekong Basin from Kratie to the South China Sea, including the Tonle Sap Lake and Floodplain, the Cambodian floodplains and the Vietnamese Mekong Delta. At the delivery of the model by Halcrow it was decided that further improvements had to be made in the model schematization and calibration. Significant improvements were indeed made in 2006 by Mr To Quang Toan of the Southern Institute for Water Resources Research (SIWRR) in Ho Chi Minh City. Adaptations and recalibration were made in the first half of 2008 by JBA Consulting. The performance of the model has been reviewed by Consultants (see Appendix 7 to Annex 1). It was concluded, that:

- the current ISIS model still has to be improved before it can be used as a reliable instrument in the study of flood management scenarios. Currently, it does not satisfy the criteria that have been set by MRCS for acceptance of the model.
- apart from differences in peak levels, which may partly be due to reference errors, the error in the celerity of flood wave propagation pose a more serious problem, leading to an approximately one week late arrival of the flood wave in the Plain of Reeds and the Long Xuyen Quadrangle.
- the current model will be acceptable for demonstration purposes to study the selected focal areas in the border area between Cambodia and Vietnam. For a final analysis the ISIS model has to be improved further.
- for the simulation of structural measures to change the nature of the floods in the project areas, adaptations in the model schematization are required. As the current model serves as a reference, any changes in the schematization and its associated parameter settings

must be introduced in a way consistent with the procedures applied in the development of the reference model.

The schematisation of the Cambodian and Vietnamese Focal Areas in ISIS is shown in Figure 4.1.

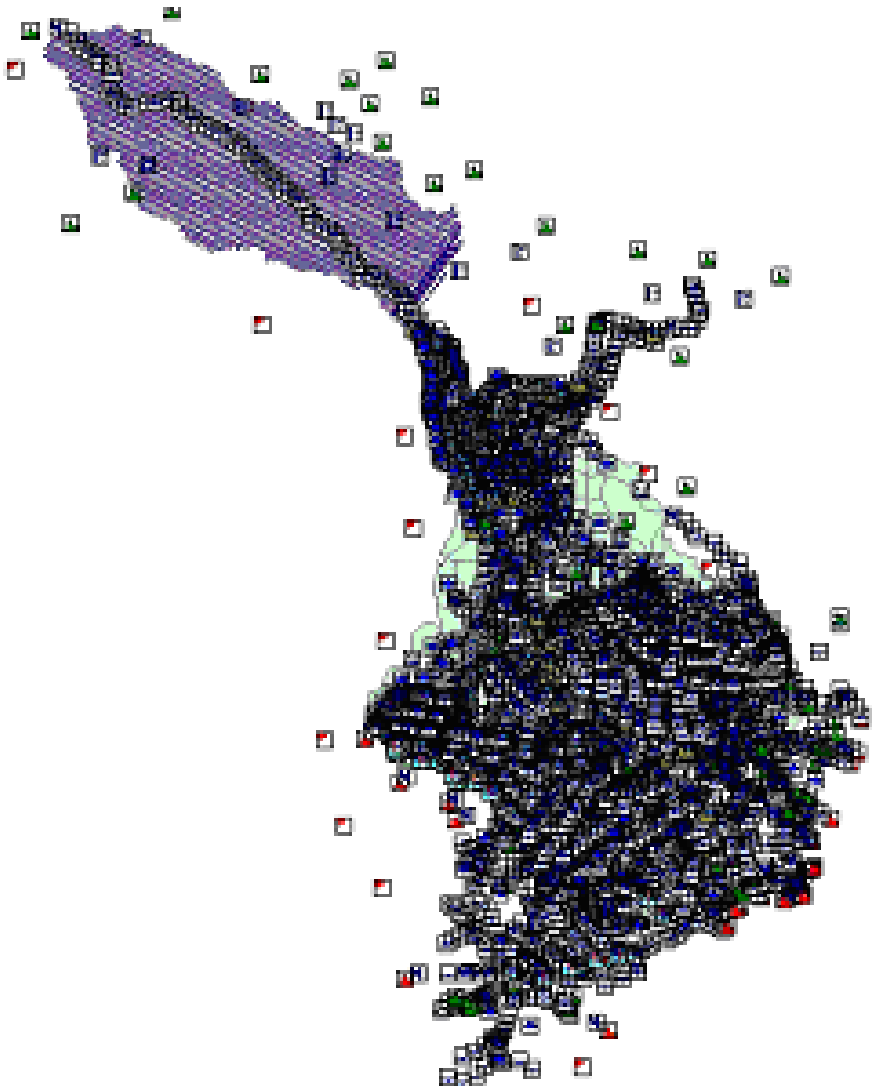

Figure 4.1 ISIS-schematisation of the Mekong delta

The Focal Areas in Vietnam have been treated in far more detail than the areas in Cambodia. To reliably simulate the effect of flood management measures in the Cambodian part of the delta a more detailed network to be implemented has been requested for. This has been done late 2008 and early 2009 but further extension of nodes is still needed, requiring surveys. Hence the effect of the alternatives for the Focal Areas in Cambodia on the flood hazard can only schematically be assessed.

4.3 Mekong at Kratie

The water level series, stage-discharge measurements and discharge series of the Mekong at Kratie have been reviewed in Annex 8. Water levels at Kratie are available since 1933. It appears that at several occasions gauge shifts have taken place and that a number of periods are of doubtful quality. Furthermore, stages at Kratie have gradually changed in the course of time, due to developments downstream. This implies that the stage-discharge relation will have changed with time. Unfortunately, between 1969 and 2002 no discharge measurements were carried out at Kratie and those carried out since 2002 with ADCP appear to be biased relative to the current meter measurements in the past. Also, the hydraulic control at Kratie is complicated and difficult to describe with shifted type power relations. This makes extrapolation beyond the measured range cumbersome. Finally, the stage-discharge relation for Kratie is affected by backwater from the Tonle Sap: for a particular water level at Kratie during rising stages when water is flowing into the Tonle Sap the discharge at Kratie is higher then during falling stages when water is flow out of the Tonle Sap. So, summing up, though the sensitivity of the gauge at Kratie is small (small dQ/dh), a number of factors make the conversion of stages into discharge uncertain.

In view of these difficulties and because for Stung Treng a longer series is available (since 1910 up to and inclusive 2006), preference has been given to the discharge series of Stung Treng. The basin area at Stung Treng measures 635,000 km^2, whereas at Kratie the upstream area is 646,000 km^2, i.e. only 1.7% larger than at Stung Treng. In the flows measured at both locations this difference is not visible. Regarding peak flows, differences are even further diminished by attenuation between Stung Treng and Kratie. For a correct reproduction of the flow at Kratie, the flow at Stung Treng has to be shifted with 1 day to account for travel time between the two sites. Still, the discontinuity in the recent series based on ADCP-measurements at Kratie remain and should be further analysed on basis of concurrent current meter and ADCP discharge measurements at Kratie.

The frequency curves of daily Mekong discharges at Stung Treng are presented in Figure 4.2. The flows are highest in August and September, with the peak value occurring around 1 September, and lowest discharges in April and early May. Note that from these graphs no information is obtained about the true shape of the hydrographs in a particular year as sequential information is not contained in the frequency curves.

Extreme value analysis has been carried out on the annual maximum peak flows and flood volumes at Stung Treng using GEV-distributions. Particularly the flood volumes are of importance for the Mekong Delta as these create the highest water levels and flood damages. The results of the extreme value analyses are shown in Table 4.1 and Figure 4.3. The correlation between the peak flows and flood volumes is included in the bivariate extreme value distribution on peak flows and flood volume. For its establishment reference is made to Appendix 9 for the details.

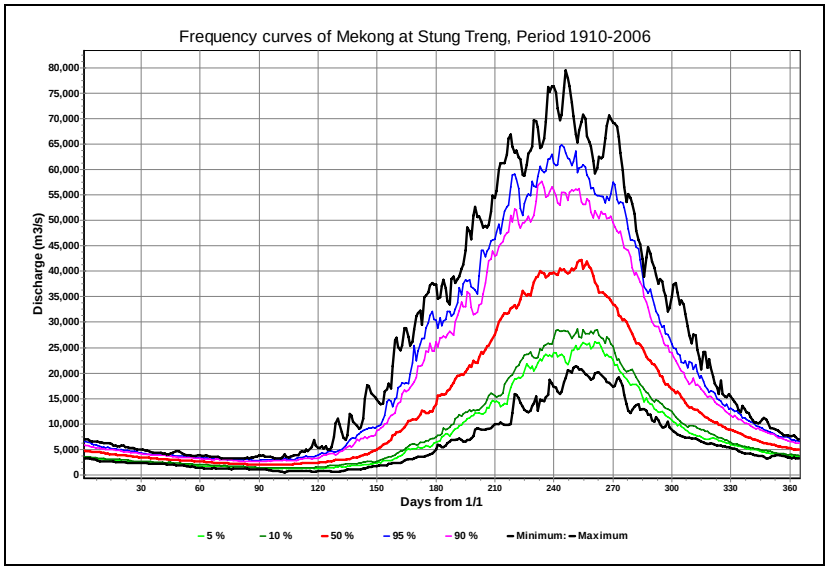

Figure 4.2 Frequency curves of the Mekong discharge at Stung Treng, Period 1910-2006

Table 4.1 Annual maximum discharge and flood volume in the Mekong at Stung Treng, period 1910-2006

T	Peak flow (m^3/s)	Flood volume (MCM)
2	54,400	331,000
5	62,600	389,000
10	66,600	416,000
25	70,600	440,000
50	72,900	453,000
100	74,800	463,000

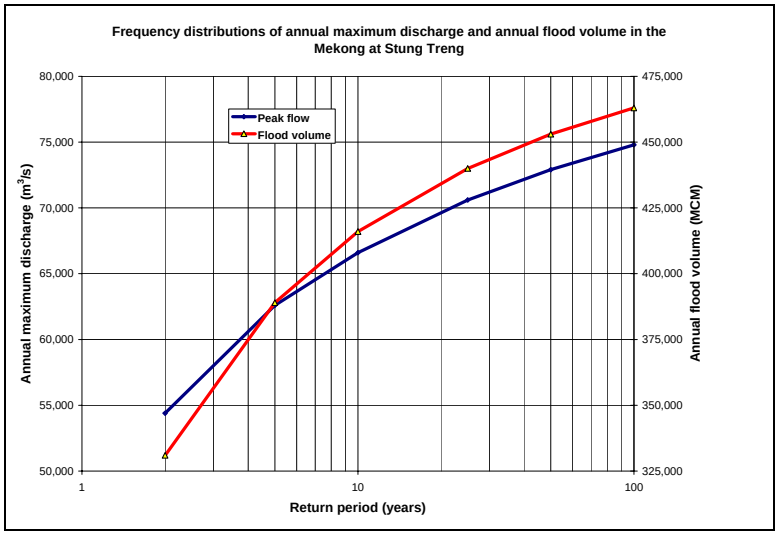

Figure 4.3 Frequency distributions of annual maximum discharge and flood volume in the Mekong at Stung Treng, Period 1910-2006

4.4 Tributary inflow to Tonle Sap Lake

The area draining to Tonle Sap up to the highways 5 and 6 amounts 68,830 km^2. It comprises the drainage areas of 13 Stungs shown in Figure 4.4. Inflow series of daily discharges are available for the years 1997-2004. A multiple regression equation has been used for the generation of monthly tributary flow of month *i* as a function of the tributary flow in month i-1 (to preserve the serial correlation) and the flow at Stung Treng in the same month (to preserve the cross-correlation). A normally distributed random number was added to preserve the variance. Unlikely numbers beyond observed values for a month were eliminated. The frequency distribution of the generated flows (aggregated to annual flows) is shown in Figure 4.5. The monthly flows were next disaggregated to daily values based on their degree of resemblance with the observed years: daily values of observed years were scaled per month to the required generated value.

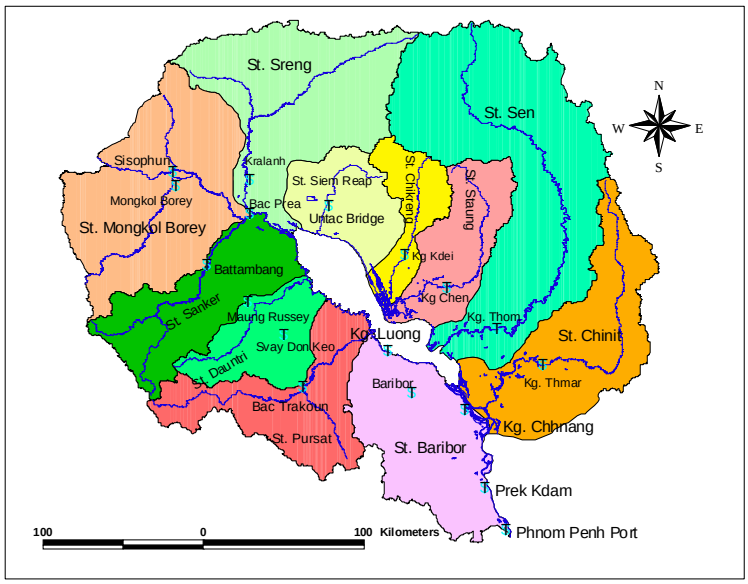

Figure 4.4 Tributaries draining to Tonle Sap Lake

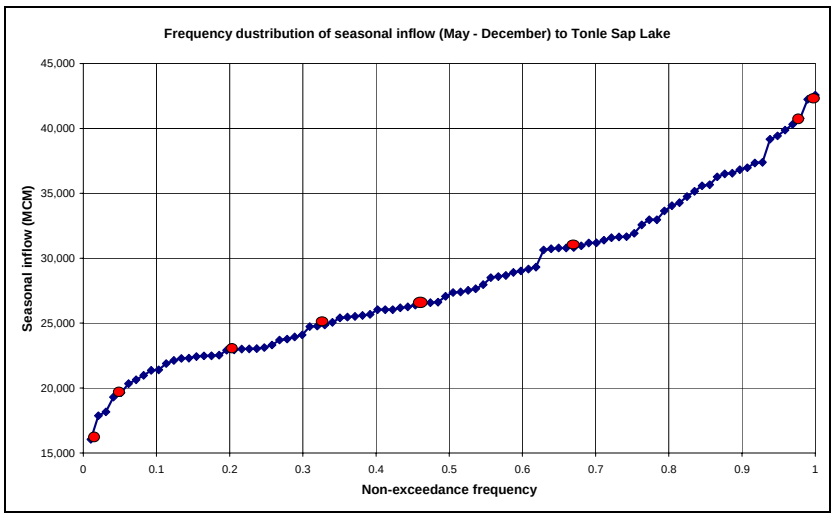

Figure 4.5 Frequency distribution of generated and observed (red dots) inflow to Tonle Sap Lake

Figure 4.6 Ton Le Sap Lake as seen from the plane, looking in south-westerly direction. The lower part of the picture shows the Siem Reap river. On the upper right side the inflow of the combined Stung Sanker/Stung Sisophun/Stung Sreng is visible.

4.5 Tributary inflow to Mekong

Apart from the inflow to the Tonle Sap Lake the Delta Model also requires inflow series for the tributaries Prek Te, Prek Chhlong, Prek Thnot, East Vaico River, and West Vaico River. The daily flow series for the period 1985-2006 are available from the DSF files created by the SWAT model. Since the SWAT-series show no correlation with the flow in the Mekong a pragmatic approach was used to extend the series by applying a block-wise repetition of the series 1985-2006 for the years 1910-1984.

4.6 Rainfall

Daily series of 9 locations in Cambodia and of 5 locations in Vietnam are required as input to the hydraulic model of the Mekong Delta. Data is available for the locations for the period 1985-2006. The annual maximum daily values generally are in the order of 100 to 150 mm, occasionally with larger values up to 400 mm in Can Tho in 1985. Analysis showed that seasonal rainfall at the selected locations hardly correlated with Tonle Sap inflow and not at all with the flow in the Mekong. Hence, a block-wise repetition of the series 1985-2006 was applied for the period 1910-1984.

4.7 Evaporation

For the same locations as rainfall is input into the model also evaporation data is required. For the locations in Vietnam daily series is available from 1985 onward with the exception of 2002. The series available for Cambodia are shorter. In case data is not available monthly averages have been applied, in view of the limited variability from year to year of potential evaporation in a particular month.

4.8 Water use

At 128 nodes in the network of the Delta model water is abstracted for agriculture, domestic and industrial use. The variation in the total abstraction varies from about 1400 m3/s in January till almost 0 m3/s at the end of September. The total annual abstraction amounts 16.5 BCM. During the flood season the demand is about 4.4 BCM in total, i.e an abstraction of less than 300 m^3/s, which is smaller then the error margin in the computed discharge from the Mekong.

4.9 Sea boundary

In total at 19 nodes water level boundaries are defined in the Delta Model. These boundaries are taken from hourly observations made at the 6 stations listed in Table 4.2.

Table 4.2 Overview of water level stations at sea boundaries

Station	River	Province	Remark
Rach Gia	Cai Lon	Kien Giang	Draining to Gulf of Thailand
Song Doc	Song Ong Doc	Ca Mau	-do-
Ganh Hao	Ganh Hao	Ca Mau/Bac Lieu	Draining to South China Sea
My Thanh	Bassac	Soc Trang/Tra Vinh	Draining to South China Sea
Ben Trai	Cua Cung Hau	Tra Vinh/Ben Tre	Southern Mekong outlet, draining to South China Sea
Vam Kinh	Cua Dai	Ben Tre/Tien Giang	Northern Mekong outlet, draining to South China Sea

The hourly observations used in the Delta Model are records of the year 2000. The characteristics of the series have been discussed in the previous chapter. This series is applied to all historical years from 1910 onward. It appears that the year 2000 slightly underestimates the range of water levels at the sea boundary. It was shown that the annual maximum daily maximum water levels are not correlated with the annual flood volume flowing into the delta. It implies that in the area influenced by the downstream boundary addition of the backwater difference between the year 2000 maximum and the long term average of the annual maximum will be sufficient. This difference at Tra Vinh is 1.69-1.62 = 0.07 m. This effect though has practically vanished in the river reaches bordering the Focal Areas.

5 Flood hazard assessment

5.1 General

5.1.1 Description of scenarios

For the management of floods and related risks in the Focal Areas in the Mekong Delta the following development scenarios have been considered:

[1] Base Case
The existing condition of land use and flood control levels in Cambodia and Vietnam.

[2] Scenario Cam0: flood protection in Cambodia
This scenario comprises of early flood protection and full flood protection in Cambodia according to recommendation in Stage 1, while no development in Vietnam is assumed. The protection in Cambodia is as follows:

- Takeo
  - Zones 1 and 3: full protection
  - Zone 2: early flood protection
- Prey Veng
  - Zone 1: early flood protection
  - Zones 2 and 3: 1: 10 year flood protection (+free board)
  - Zone 4: no protection.

Early flood protection is defined as follows: based on the model simulation of the base case the annual maximum water level of the early flood season, which ends on August 1, is derived for the series of 97 years (1910-2006). Subsequently, the water level with a return period of 10 years, $h_{1Aug;\ 10}$, is derived from this series. So $h_{1Aug;\ 10}$, is the water level that is exceeded on average once in every 10 early flood seasons (1 May – 1 August). Early flood protection means that the crest height of the dikes are raised to the level of $h_{1Aug;\ 10}$. This means the probability of flooding in the early flood season is equal to 1/10 (10%).

[3] Scenario Vna flood protection in Vietnam, variant a
This scenario comprises of early flood protection and full flood protection in Vietnam.

- Long Xuyen Quidrangle
  - enlargement of canals,
  - no sluices along Bassac,
  - rubber dams open on the 15th of August
- Trans Bassac: full protection as at present
- Plain of Reeds: Canal enlargement

[4] Scenario Vnd flood protection in Vietnam, variant d
This scenario comprises of full flood protection in the largest part of the Mekong Delta in Vietnam. It is explicitly noted that this scenario is not in accordance with the current policy of Vietnam for flood protection of the delta. However, it provides an outlook in the far

future, say 2060 in case that the socio-economic situation might have changed so much that full flood protection would be an option.

[5] Scenario Cam0Vna: flood protection in Cambodia and Vietnam
This is the combination of scenarios Cam0 and Vna

[6] Scenario diversion:
This is the scenario in which a Diversion to the Tonle Sap lake is built for early flood control

5.1.2 Outline

Section 5.2 describes the probabilistic method that has been applied to derive probabilities of exceedance for water levels for the various scenarios. The results for the base case are presented in Sub-section 5.3. The outcomes for the development scenarios [2] – [5] are dealt with in Sub-section 5.4 and are compared with the base case, to assess the effect of the measures. Subsection 5.5 describes the effects of scenario [6]. Finally, in Sub-section 5.6 the effect of sea level rise is analysed.

5.2 Probabilistic analysis

5.2.1 Annual maximum water levels

For the probabilistic analysis for the Mekong delta downstream of Kratie we make use of the fact that a relatively long series of observed and reconstructed discharges is available for the Mekong at location Stung Treng and also for the tributaries of the Mekong downstream and the tributaries of the Tonle Sap Lake, see Appendix 9. The series, which cover the period 1910-2006, are used as boundary conditions for a hydrodynamic model (Isis) to derive a 97-year series of water levels in the flood-prone areas. The relevant statistics like probabilities of flooding and related damages can be derived directly from these series of water depths as will be demonstrated in this section.

This approach can be considered as a special case of the crude Monte Carlo simulation technique (see appendix 10). Generally, in Monte Carlo analysis a long series of all random variables is generated by taking samples from their respective distribution functions. In this case (reconstructions of) actual observations are used. Then, as in crude Monte Carlo analysis, for each sample (year) maximum water levels and flood damages are derived. From these series, exceedance probabilities of maximum water levels and flood damages are derived, using Gringortens formula:

$$p_i = \frac{r_i - 0.44}{N + 0.12} \qquad (5.1)$$

where:
p_i = probability of exceedance of the annual maximum water level in year *i*
N = total number of years
r_i = rank number of the maximum water in year *i* (1 = highest, n = lowest)

The annual maximum level in a large number of model output nodes (3445) was derived and analysed. Figure 5.1 shows an example of the results for a single node. It shows annual maximum water levels plotted against year of occurrence (above) and estimated probability of exceedance (below).

The observations in Figure 5.1 are connected by a red dotted line, which assumes the relation between the logarithm of the exceedance probability and the water level to be linear in between observations. This line is used to derive the water level for return periods of 2, 5, 25 and 100 years.

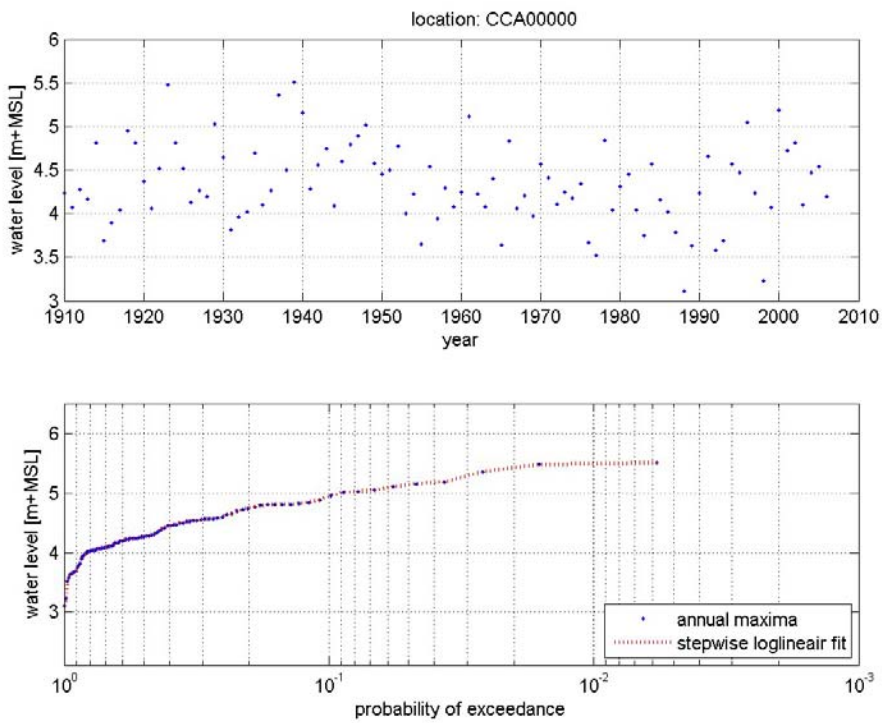

Figure 5.1 Derived annual maximum water levels at output node CCA0000 plotted against year of occurrence (above) and estimated probability of exceedance (below).

Since the series of annual maxima is close to 100 years, the estimated 100-year water level is by definition approximately the same as the maximum observed water level. This can be seen in Figure 5.1, where the red line crosses the 10^{-2} – probability line at approximately the same level as the blue dot to the far right (the maximum observed water level). The estimated 100-year water level in this case is equal to MSL+5.49 m, the maximum observed water level is equal to MSL+5.51. Figure 5.2 compares the estimated 100-year water level with the observed maximum water level for all 3445 locations. All locations are very close to the line x=y, showing the difference between the 100-year water level and the observed maximum water level is small. For 7 locations the difference is more than 20 cm, which may be suspicious. A closer look, however, revealed that there seems to be nothing wrong with these locations. These are just examples of cases where the highest annual maximum water level differs significantly from the second highest annual maximum water level. These 7 locations are all in the same area and the years of occurrence of the highest and second highest annual maximum are the same for all locations.

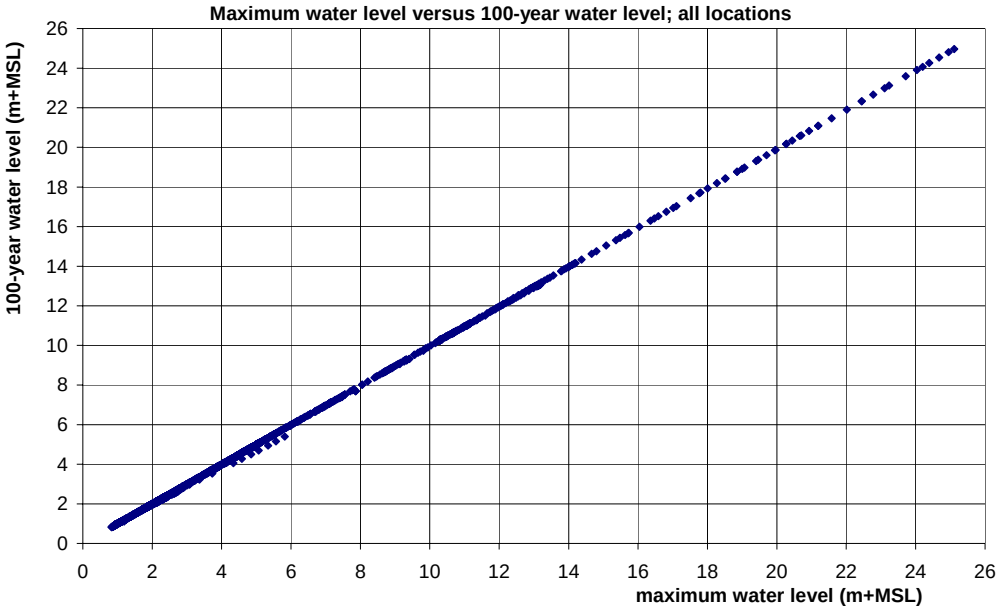

Figure 5.2 Comparison of the derived 100-year water level (horizontal axis) and the maximum water level in the period 1910 – 2006 at 3445 locations all over the lower Mekong basin.

For the remainder of the analysis it is relevant to know what causes the highest water levels to occur at the various locations. Of course, in this area the discharge of the Mekong river is the main driving force, but we need to identify the years and the corresponding flow conditions that lead to high water levels. Furthermore, it is relevant to know whether or not this varies from location to location, i.e. at some locations the peak discharge may be most relevant, whereas for other locations high flow volume might be the number 1 cause of high flood levels.

Table 5.1 shows the years in the period of 1910-2006 in which extremely high water levels occurred at a relatively large amount of locations (model nodes). The table shows years that are ranked highest, second highest or third highest at a relatively large amount of many locations. The numbers should be interpreted as follows: e.g. in 1228 model nodes the maximum water level was highest over the period 1910-2006 in the year 1939. And in 1068 model nodes the water level was third highest over the period 1910-2006 in the year 1937.

Table 5.1 Years with highest, second highest or third highest water levels over the period 1910-2006 in a relatively large amount of locations. E,g in 1228 model nodes the maximum water level was highest over the period 1910-2006 in the year 1939.

highest peak		second highest peak		third highest peak	
year	**# locations**	**year**	**# locations**	**year**	**# locations**
1939	1228	1923	833	1937	1068
1937	834	1937	458	1961	383
1952	372	1996	410	1923	324
1996	293	1939	378	2000	316

For each year in the period 1910-2006 the annual peak discharge and annual flow volume of the Mekong river at Stung Treng was derived. The flow volume in this analysis is defined as the total flow above a threshold discharge of 25.000 m^3/s, the latter being approximately the flow capacity of the Mekong river near Phnom Penh. Figure 5.3 shows a scatter plot of volumes vs. peak discharges. It shows, not surprisingly, there is a positive correlation between volume and peak discharge.

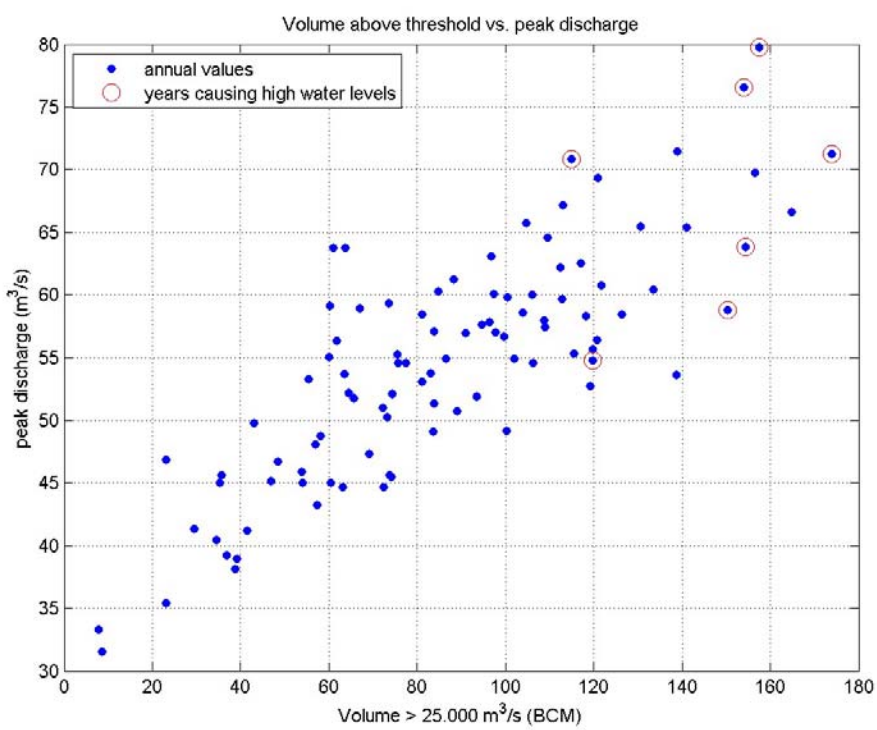

Figure 5.3 Volume of flow above the threshold of 25.000 m^3/s versus peak discharge

The seven years of Table 5.1 (1923, 1937, 1939, 1952, 1961, 1996 and 2000) are circled in red in Figure 5.3. These red circles are generally in the upper right corner of the figure, confirming the fact that a combination of high flow volume and high peak discharge in the Mekong river leads to high water levels in the flood-prone areas. In order to find out which one of those two is the most relevant variable, scatter plots were produced in which both variables were plotted against water levels in the flood-prone areas. Figure 5.4 shows the scatter plot of the annual flow volume in the Mekong versus the annual maximum water level at model node BAT39000. Figure 5.5 shows a similar plot for the peak discharge. Both figures clearly show a positive correlation as can be expected. The correlation for the flow

volume is significantly stronger than for the peak discharge. This is a very typical example, correlations like these are found at many model nodes. This indicates that the flow volume is more relevant than the peak discharge with respect to generation of high water levels in the flood prone areas.

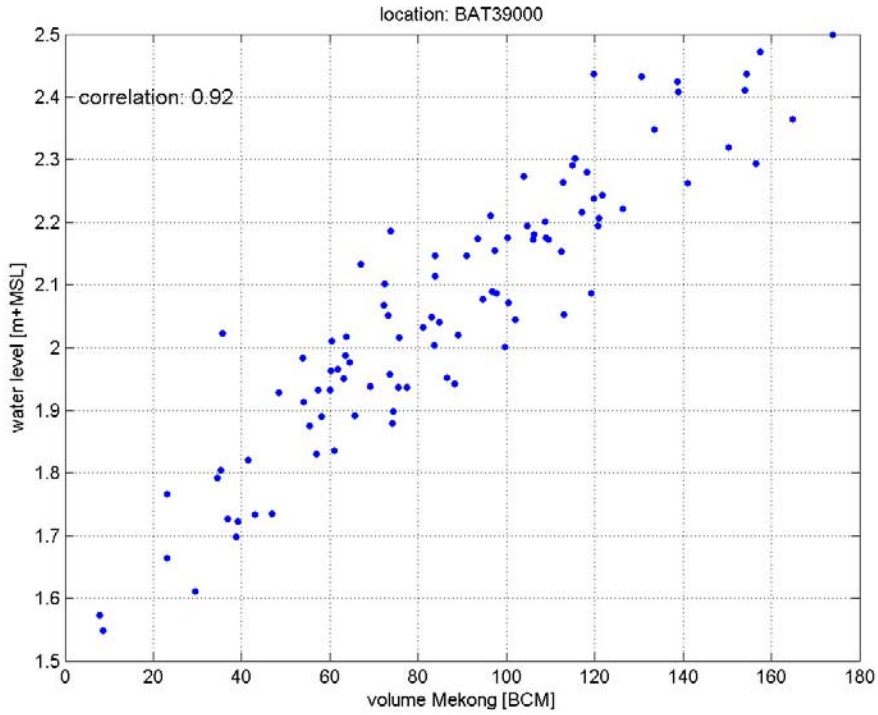

Figure 5.4 Annual flow volumes (BCM) in the Mekong river at Stung Treng above a threshold discharge of 25,000 m^3/s versus annual maximum water level at model node BAT39000.

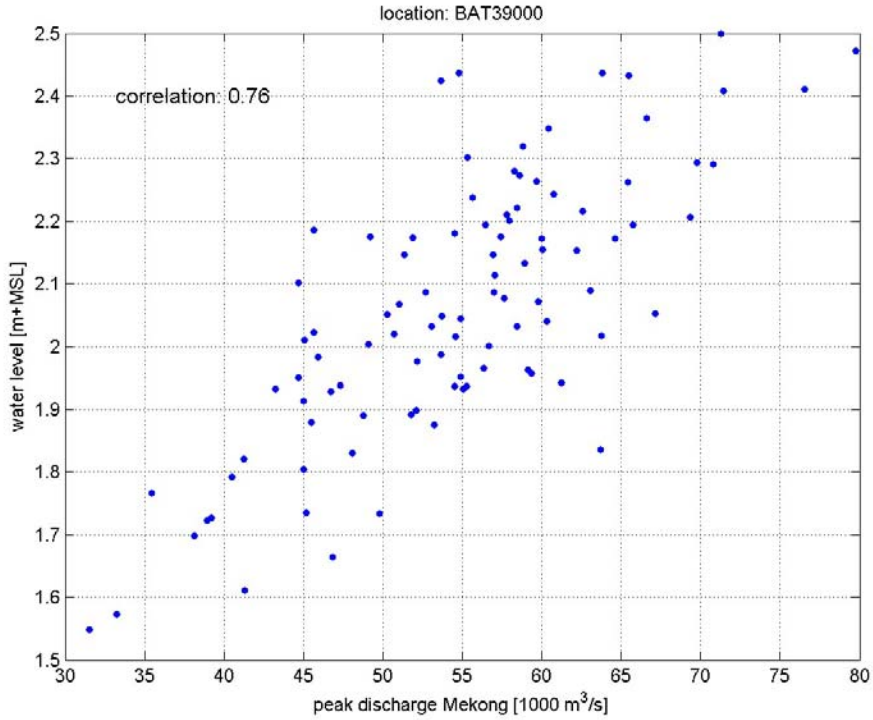

Figure 5.5 Annual peak discharges (1000 m^3/s) in the Mekong river at Stung Treng versus annual maximum water level at model node BAT39000.

5.2.2 Maximum water levels in the early flood season

The previous pages describe the probabilistic analysis for the annual maximum water level in flood plain areas. For agriculture, the maximum water level during the early flood season (1 May - 1 August) is generally more relevant than the annual maximum water level. If the area is flood free during the early flood season, the crops can be safely harvested. For agriculture, a flood hazard assessment for the early flood season is required as well. The procedure for this is similar to the procedure of section 5.2.1. The only difference is that the maximum water level in the period (1 may – 1 August) is derived for each year in the period 1910-2006, instead of the annual maximum water level.

5.2.3 Fitted function

For practical purposes it is convenient to derive a fit for the relation between water level and its corresponding probability of exceedance. These fitted functions are used to derive the annual expected damage (see for example Volume 2B and Volume 3A). Analysis showed that the shifted exponential function is generally a good description of this relation:

$$h(p) = ae^{bp} + c \qquad (5.2)$$

where:

h = water level
p = probability of exceedance
a,b,c = fit parameters
e = 2.718282 …

The parameters a,b,c, are location specific and based on fits of the available data from simulations with Isis. Figure 5.6 shows an example of a fitted function.

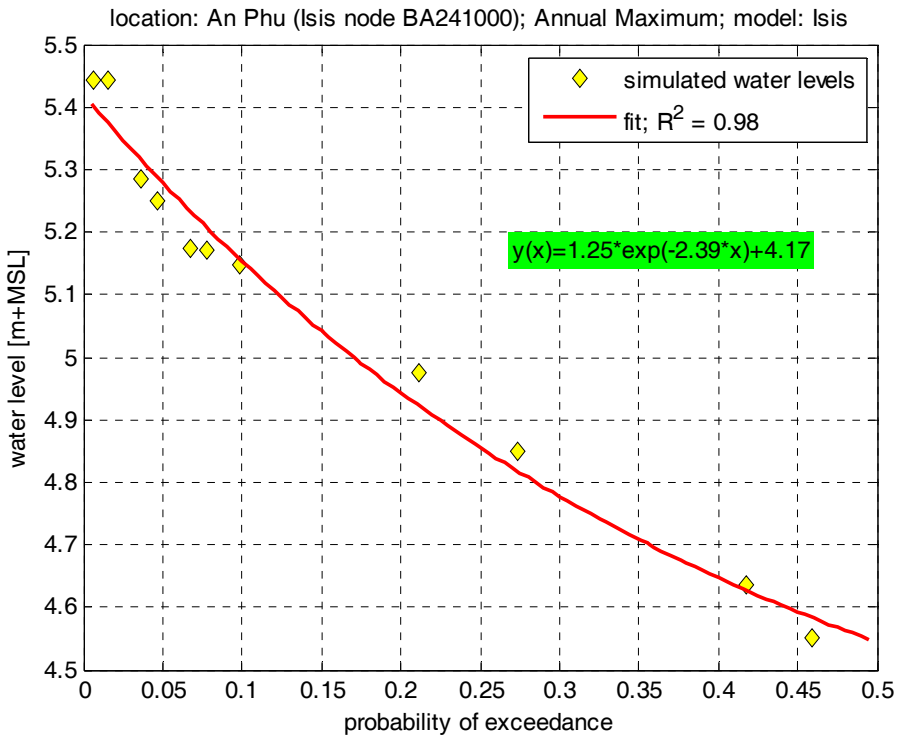

Figure 5.6 Fitted function of probability of exceedance for water levels for location An Phu; Base case.

In some cases the shifted exponential function is not good description of the relation between water level and probability of exceedance. This is mainly the case for locations for which water levels with low probabilities of exceedance are much higher than the more regularly occurring water levels. In these cases the power function is a very good alternative:

$$h(p) = ap^b + c \tag{5.3}$$

5.3 Resulting flood maps for the Base Case

Flood frequency curves like Figure 5.1 were derived for all 3419 output nodes of the hydraulic model. The water levels for 2, 5, 10, 25 and 100 years were subsequently compared with ground elevation to determine flood depth and extent. Attachments 1.1 to 1.5 show the 2, 5, 10, 25 and 100-year water level for the entire Mekong delta, based on analysis for the *entire* flood season. Attachments 1.6 to 1.10 show the 2, 5, 10, 25 and 100-year water level for the entire Mekong delta, based on analysis for the *early* flood season.. Annual maximum water levels generally occur in the period August – November, so the maximum water level in the early flood season is generally significantly lower than the annual maximum water level.

It is very important to realise that the maps do not show the water levels that occur during a single extreme event and are therefore made up of highest water levels from several years combined.

The complete set of flood hazard maps for the scenarios has been provided on DVD. These maps have also been included in Volume 6E, together with maps showing the differences in flood depth between a scenario and the base case.

5.4 Results for development scenarios [2]-[5]

5.4.1 Hydraulic model output

Each scenario as described in section 5.1.1 is simulated with the Isismodel to compare resulting water depths and water levels with those derived for the base case. The effects of the scenarios on water levels are analysed in detail for 59 locations, each representative of one of the 59 districts in the Delta area. Of these 59 districts, 34 are located in Vietnam and 25 in Cambodia. Furthermore, also the effect on water levels along the Mekong and Bassac will be described in the remainder of this report.

It is noted that in the available hydraulic model of the Mekong Delta the density of the network is insufficient for detailed simulation of flooding under the Scenarios 2 and 3 in Focal Areas Takeo and to a lesser extent in Prey Veng. Consultants requested in April 2008 for a denser network in those areas to the modelling team responsible for the recalibration (see Appendix 7). This adaptation was carried out late 2008 and early 2009 but the number of extended cross sections and reservoirs remain by far insufficient. As a consequence, we were unable to find proper representative locations for a number of districts in the West Bassac and East Mekong, particularly in the flood plains of the northern part Takeo Area and to a lesser extent in Prey Veng.

5.4.2 Estimating flood hazards from 11 simulated years

Instead of running the hydraulic model for the above scenarios for the full 97 flood seasons, only 11 selected years (1918, 1923, 1927, 1929, 1939, 1940, 1971, 1994, 1996, 2000 and 2001) were simulated in order to save valuable computation time. The years were selected in such a way that they represent the range from moderate to extreme years in terms of Mekong flows and, consequently, flood depths. However, the ranking of years in terms of high water levels differs for different locations, so it is not possible to award a specific exceedance frequency to a specific year without knowing which location is involved. Therefore, for each location separately the following procedure was applied:

1. For each of the 11 years the water level in the base case (scenario [1]) is derived (either annual maximum water level or maximum water level up to August 1)
2. The frequency of exceedance of the 11 years for the specific location is derived, based on the water level of step 1.
3. Water levels of the base case and the scenario are compared for the selected 11 years (see e.g. Figure 5.7). The water levels are plotted against the derived frequencies of step 2 to see if the change in water level is different for floods of different magnitudes.
4. The water levels with probability of exceedance of 50%, 20%, 10%, 4%, 2% and 1% (i.e. return periods of 100, 50, 25, 10, 5 and 2 years) are derived from the water levels of the 11 simulated years through interpolation.

5. A fit of the relation between water level and corresponding probability of exceedance is derived (see e.g. Figure 5.8), which can be used to derive expected annual damages.

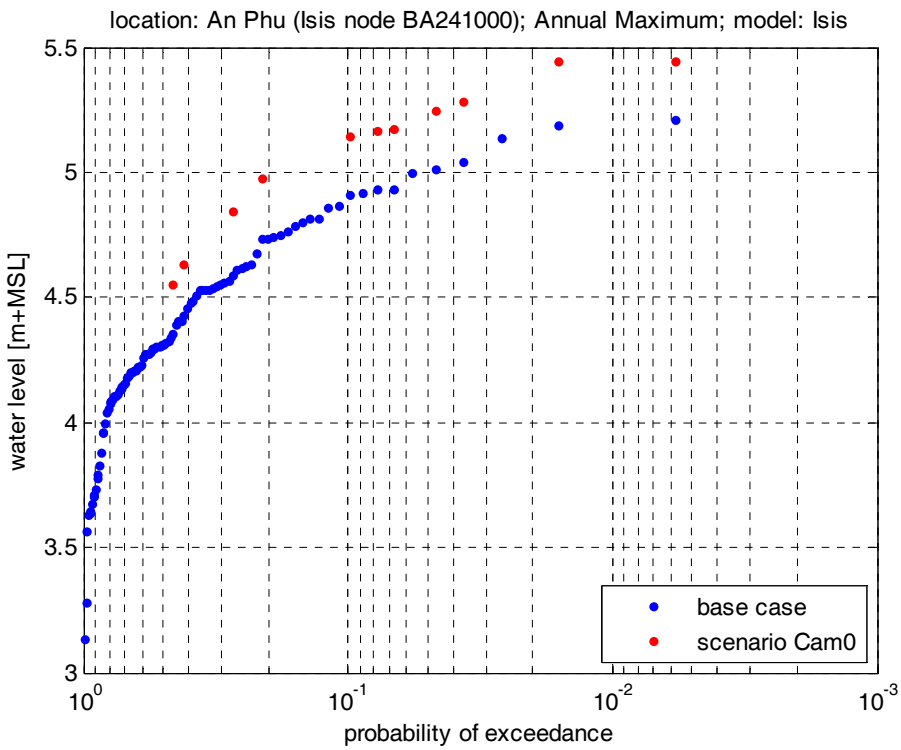

Figure 5.7 Exceedance frequencies of annual maximum water levels of 97 in the base case (blue dots) compared to water levels in 11 selected years.

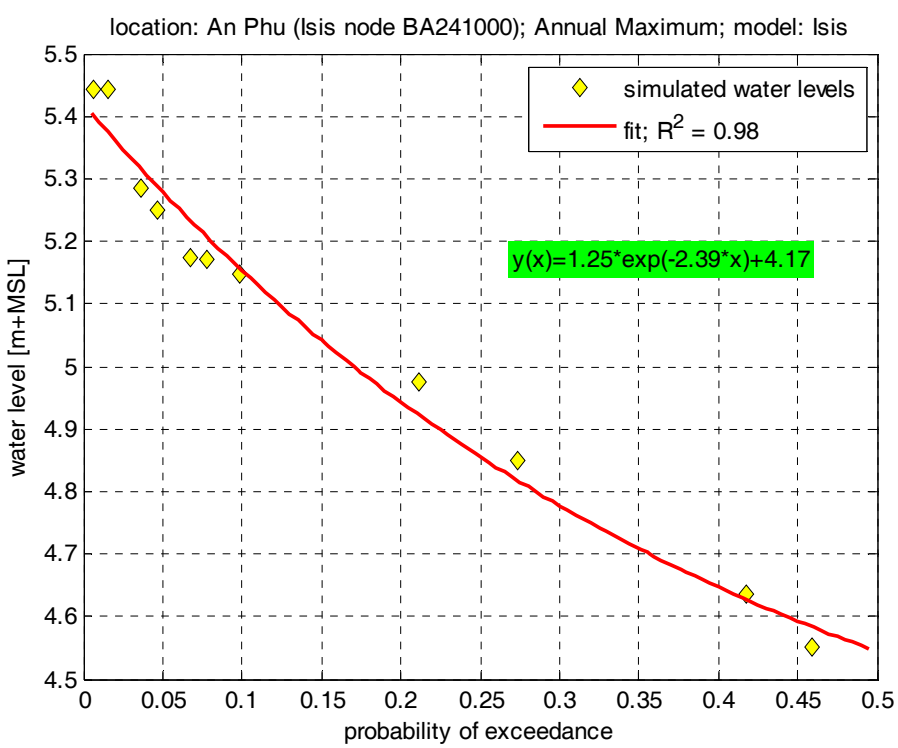

Figure 5.8 Fitted function of probability of exceedance for water levels for location An Phu; scenario Cam0

The fact that for the scenario's the results of only 11 simulation years are used may mean that the derived water levels for a given probability of exceedance are less accurate than for the base case for which 97 years have been simulated. In other words; the outcome based on 11 years is an approximation of the outcome that would have been obtained if the full 97 years would have been simulated. In order to find out what the magnitude is of the error which is introduced by this approximation, a comparison is made between the results based on 97 years and 11 years respectively. This comparison is executed for the base case, since that is the only scenario for which the full set of 97 years have been simulated. Figure 5.9 compares the resulting 100-year water levels for 59 locations. For all locations the approximation (vertical axis) is very close to the initial result based on 97 years (horizontal axis), because all points are close to the line y=x. The maximum difference between the two is 0.12 m. This means the error introduced with the approximation method is small.

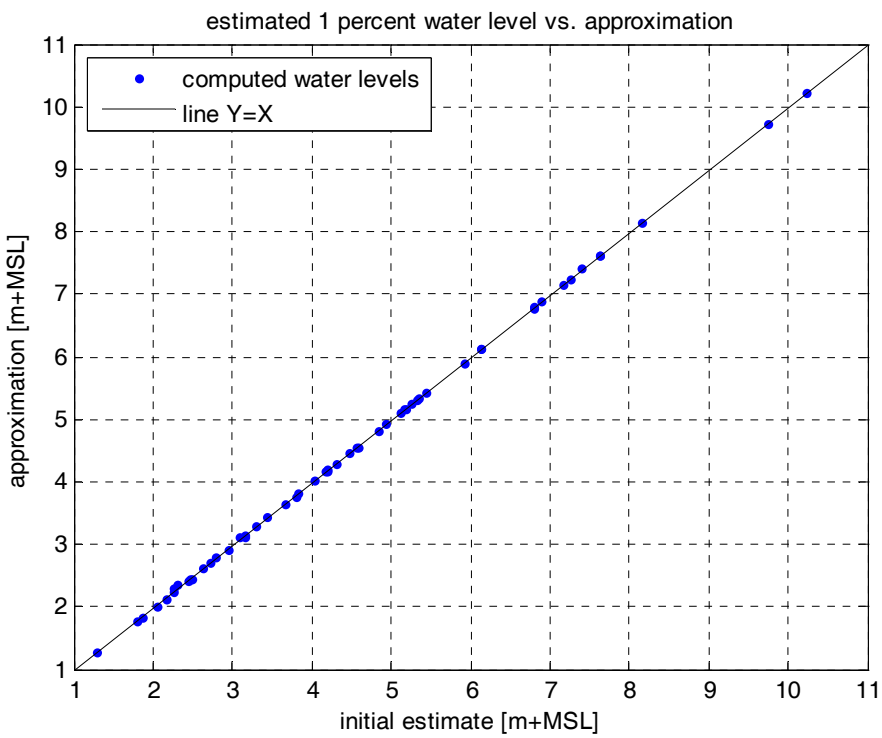

Figure 5.9 Comparison of the estimated 1%-water level (i.e. the 100 year water level) based on 97 simulated years (horizontal axis) and the approximated estimate based on 11 simulated years (vertical axis). The comparison is made for the 59 selected locations.

5.4.3 Results for scenario [2] – Cam0

The water levels with probability of exceedance of 50%, 20%, 10%, 4%, 2% and 1% for this scenario are compared with the corresponding water levels for the base case. Figure 5.10 and Figure 5.11 show the differences with the base case for the 25 locations in Cambodia and 34 locations in Vietnam respectively. As can be seen there is no consistent pattern. For 16 out of 25 locations in Cambodia the water level decreases as a result of the measures of scenario Cam0, for 8 locations the water levels increases and for one location (Preah Sdech) both

increases and decreases are observed. Of the 34 Vietnamese locations, 11 show an increase in water levels, 13 show a decrease in water levels and 10 show hardly any change at all. So for some locations the annual expected damages will increase as a result of the measures of scenario Cam0 and for some locations the water levels will decrease. This will be quantified in Volume 6E.

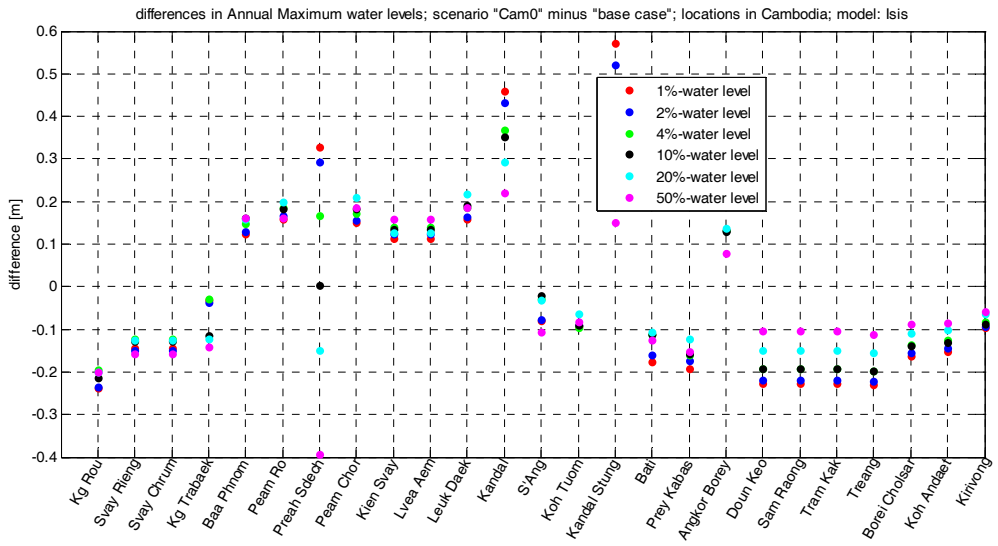

Figure 5.10 Change in the p-percent annual maximum water level (p=1, 2, 4, 10, 20 and 50) for 25 locations in **Cambodia**; comparison of scenario **Cam0** with the base case. Positive values indicate an increase in water level.

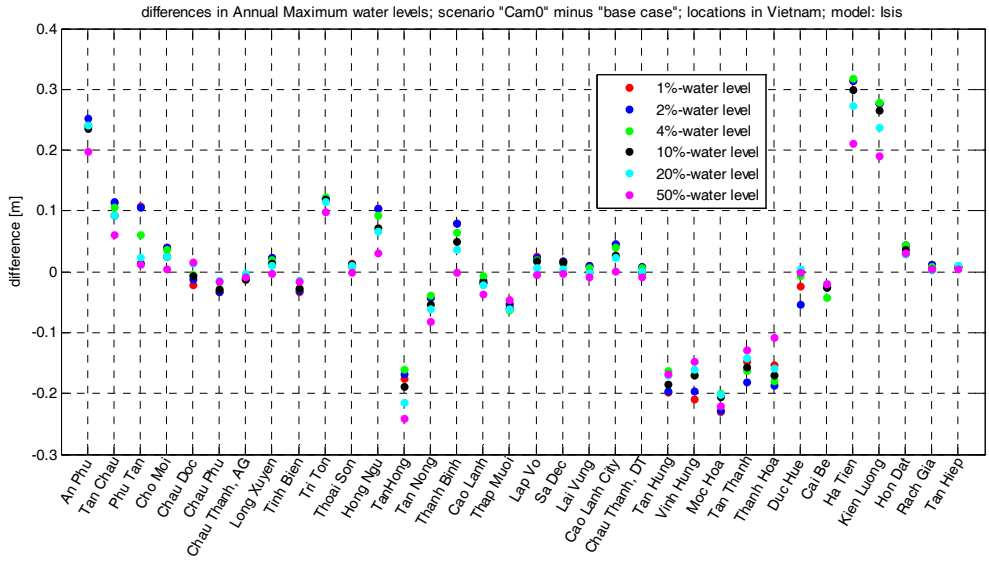

Figure 5.11 Change in the p-percent annual maximum water level (p=1, 2, 4, 10, 20 and 50) for 34 locations in **Vietnam**; comparison of scenario **Cam0** with the base case. Positive values indicate an increase in water level.

Figure 5.12 - Figure 5.15 compare water levels in the Mekong and Bassac rivers for the base case and scenario Cam0. Most noteworthy is the fact that the scenario leads to a reduction in water levels over some stretches of the Bassac river.

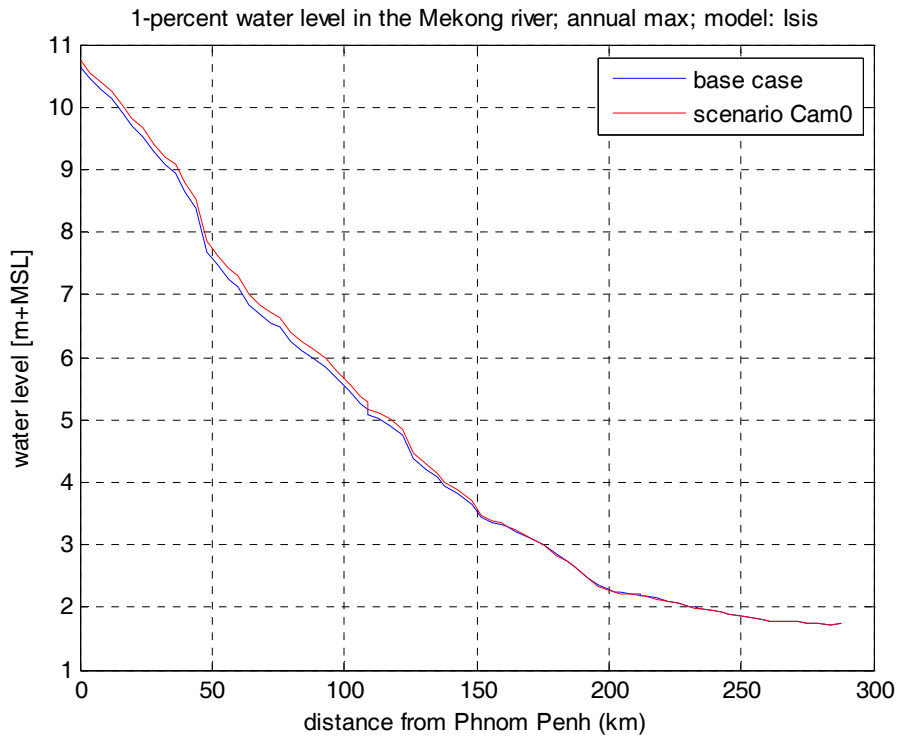

Figure 5.12 Water levels in the **Mekong** river downstream of Phnom Penh; comparison between the base case and scenario **Cam0**.

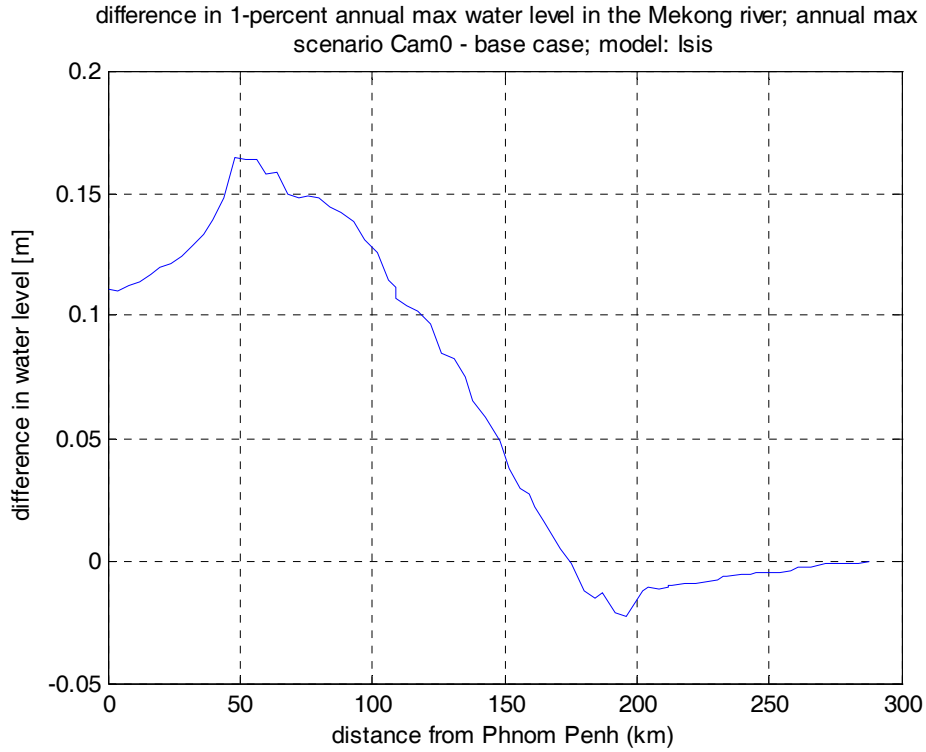

Figure 5.13 Increase in water level in the **Mekong** river downstream of Phnom Penh as a result of scenario **Cam0** (differences between the two cases of Figure 5.12).

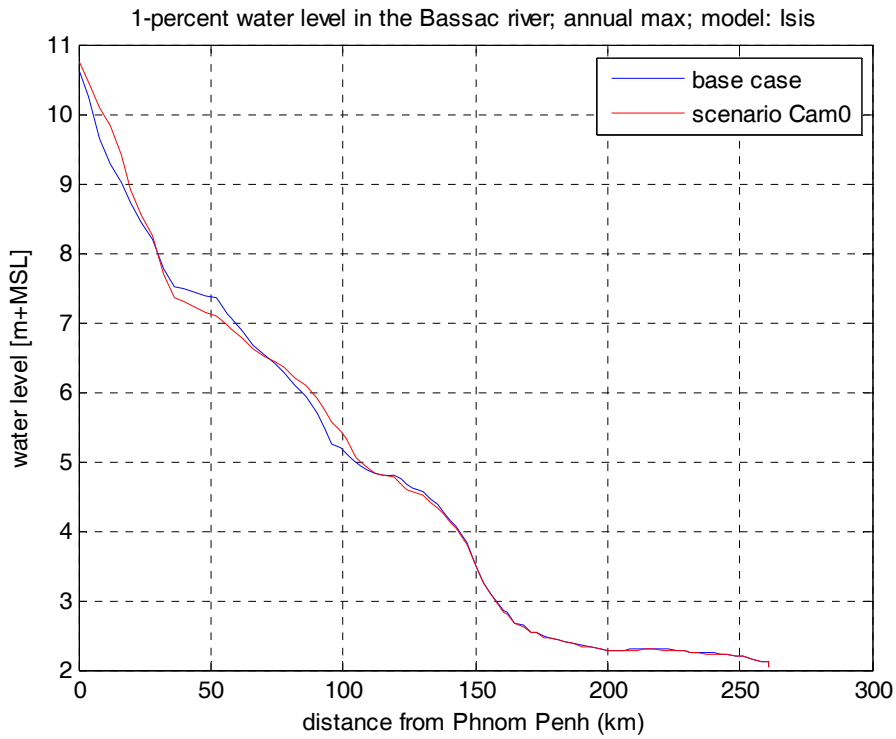

Figure 5.14 Water levels in the **Bassac** river downstream of Phnom Penh; comparison between the base case and scenario **Cam0**.

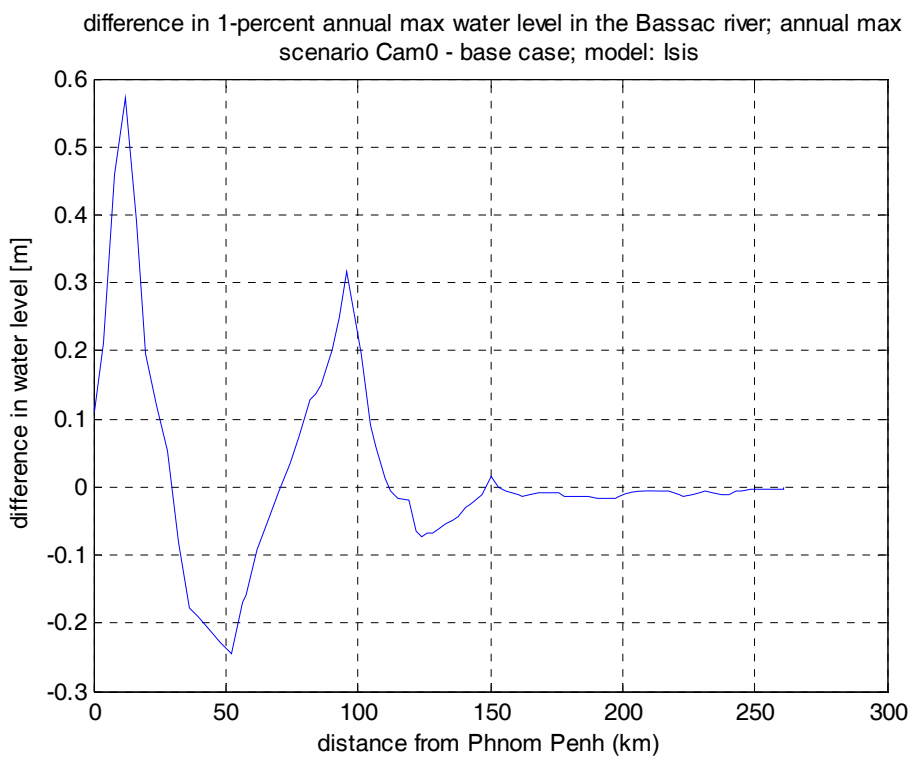

Figure 5.15 Increase in water level in the **Bassac** river downstream of Phnom Penh as a result of scenario **Cam0** (differences between the two cases of Figure 5.14).

5.4.4 Results for Scenario [3] – Vna

Figure 5.16 and Figure 5.17 show the differences in water levels between scenario Vna and base case for the 25 locations in Cambodia and 34 locations in Vietnam respectively. Again, for some locations the water levels increase as a result of the measures of scenario Vna, while for other locations the water levels decrease. All Cmabodian locations show an increase in water level. Figure 5.18 - Figure 5.21. compare water levels with probabilities of exceedance of 1% in the Mekong and Bassac rivers for the base case and scenario Vna

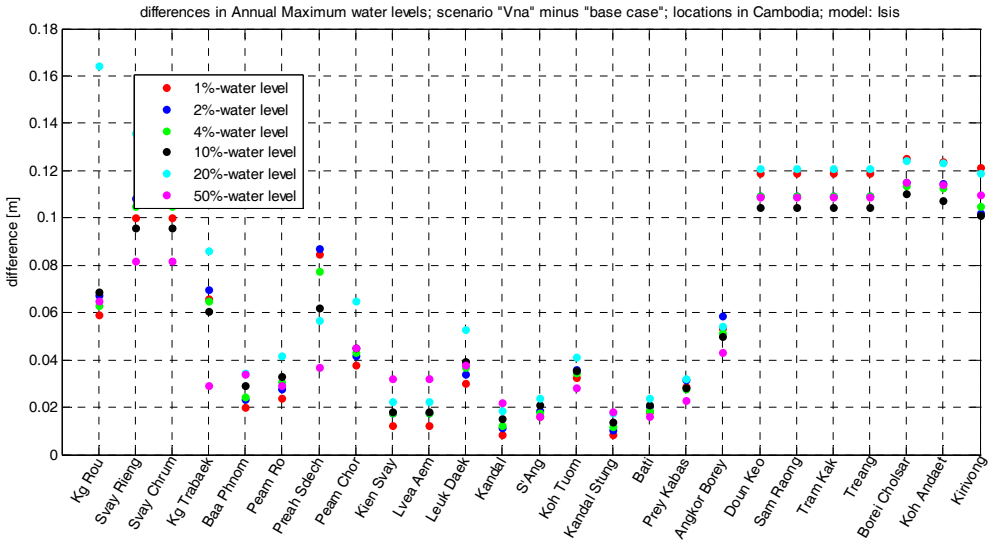

Figure 5.16 Change in the p-percent annual maximum water level (p=1, 2, 4, 10, 20 and 50) for 25 locations in **Cambodia**; comparison of scenario **Vna** with the base case. Positive values indicate an increase in water level.

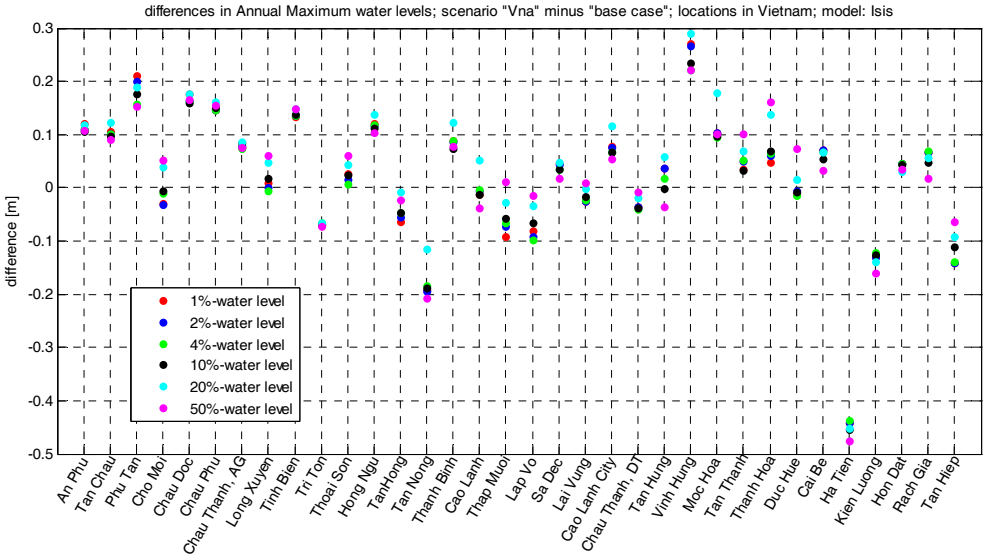

Figure 5.17 Change in the p-percent annual maximum water level (p=1, 2, 4, 10, 20 and 50) for 34 locations in **Vietnam**; comparison of scenario **Vna** with the base case. Positive values indicate an increase in water level.

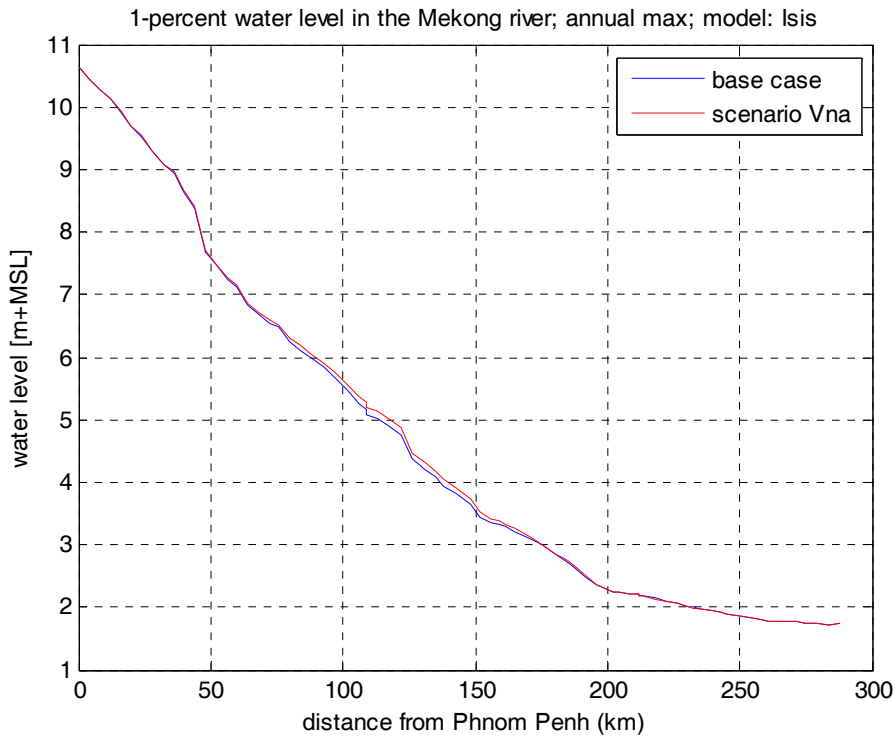

Figure 5.18 Water levels in the **Mekong** river downstream of Phnom Penh; comparison between the base case and scenario **Vna**.

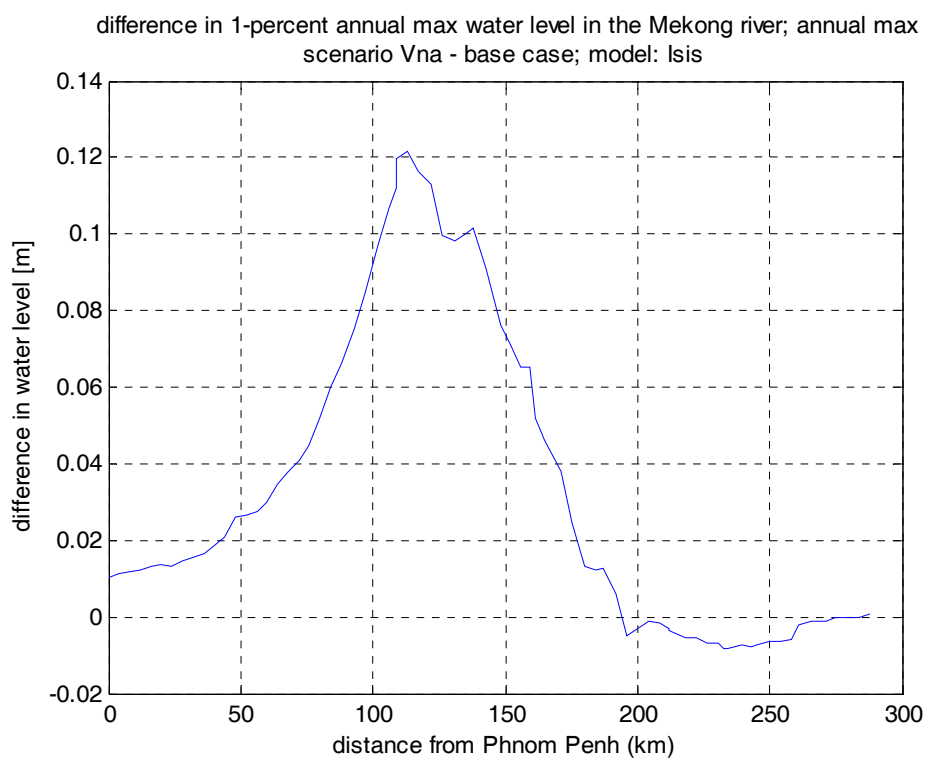

Figure 5.19 Increase in water level in the **Mekong** river downstream of Phnom Penh as a result of scenario **Vna**.

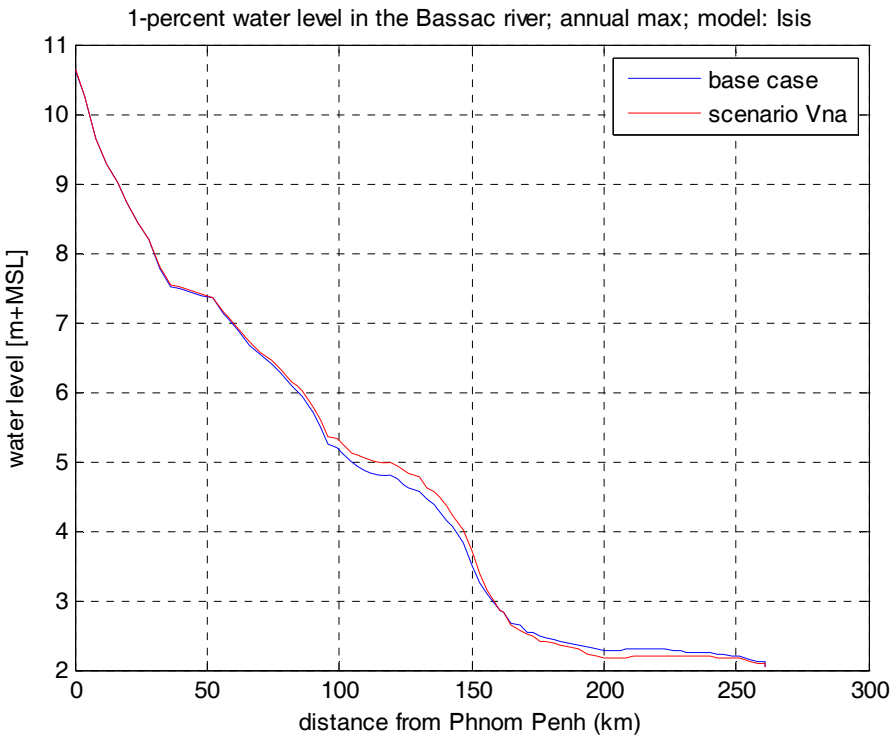

Figure 5.20 Water levels in the **Bassac** river downstream of Phnom Penh; comparison between the base case and scenario **Vna**.

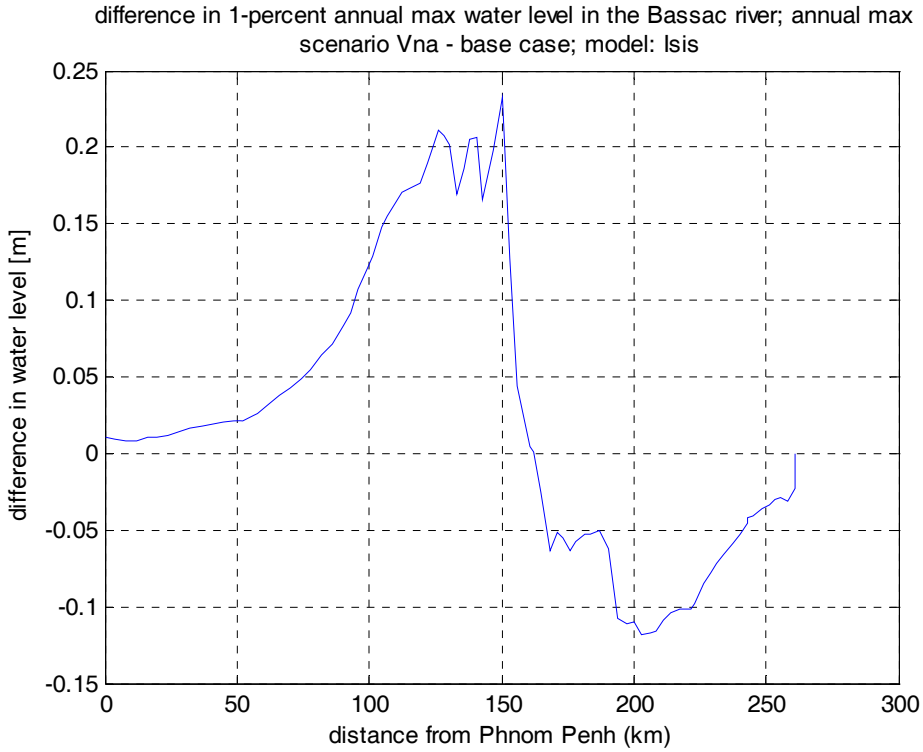

Figure 5.21 Increase in water level in the **Bassac** river downstream of Phnom Penh as a result of scenario **Vna**.

5.4.5 Results for Scenario [4] – Vnd

Figure 5.22 and Figure 5.23 show the differences in water levels between scenario Vnd and base case for the 25 locations in Cambodia and 34 locations in Vietnam respectively. Again, for all locations in Cambodia the water levels increase as a result of the measures of scenario Vnd. For locations in Vietnam the effects of changes are mixed. Figure 5.24 - Figure 5.27. compare water levels with probabilities of exceedance of 1% in the Mekong and Bassac rivers for the base case and scenario Vnd.

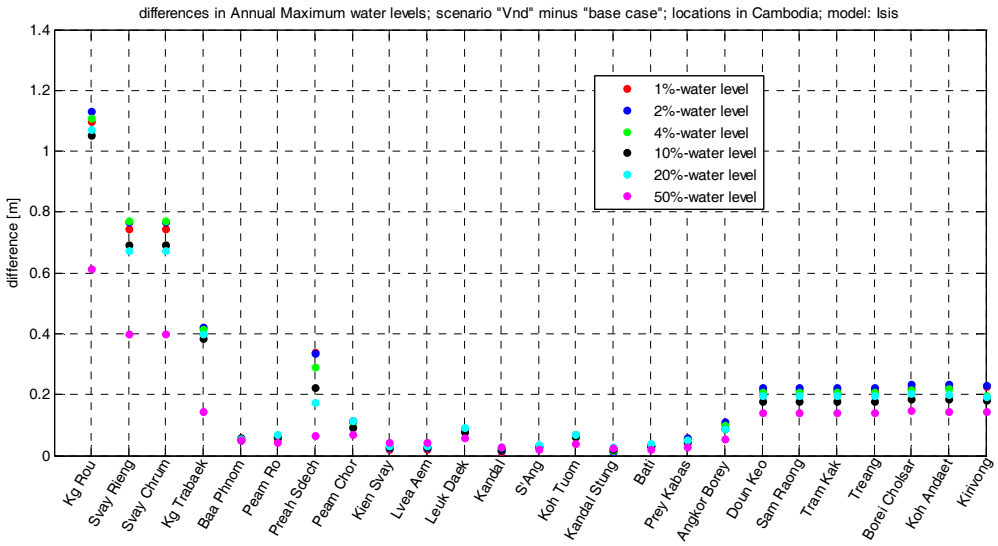

Figure 5.22 Change in the p-percent annual maximum water level (p=1, 2, 4, 10, 20 and 50) for 25 locations in **Cambodia**; comparison of scenario **Vnd** with the base case. Positive values indicate an increase in water level.

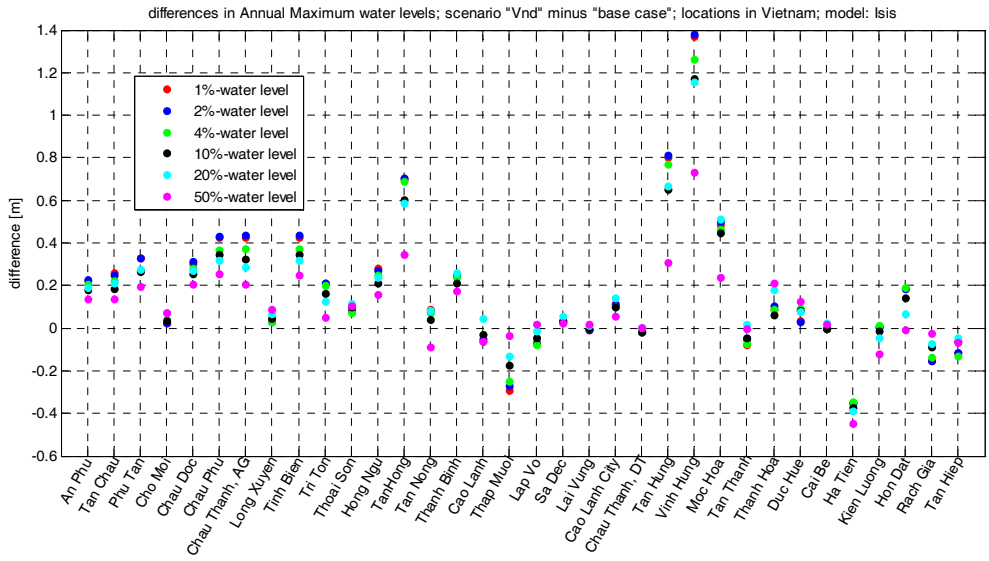

Figure 5.23 Change in the p-percent annual maximum water level (p=1, 2, 4, 10, 20 and 50) for 34 locations in **Vietnam**; comparison of scenario **Vnd** with the base case. Positive values indicate an increase in water level.

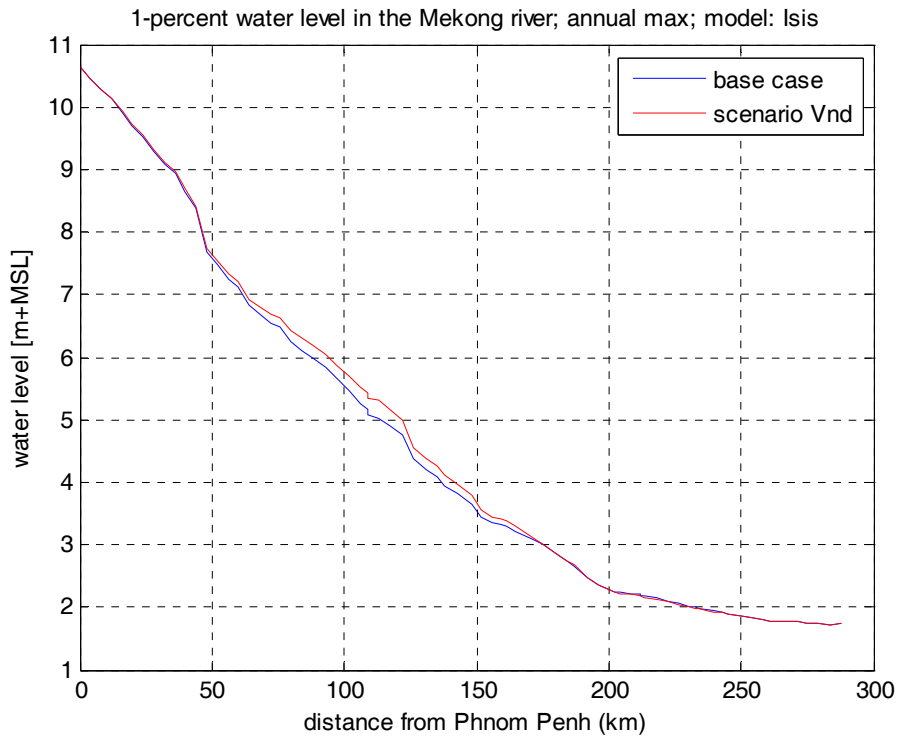

Figure 5.24 Water levels in the **Mekong** river downstream of Phnom Penh; comparison between the base case and scenario **Vnd**.

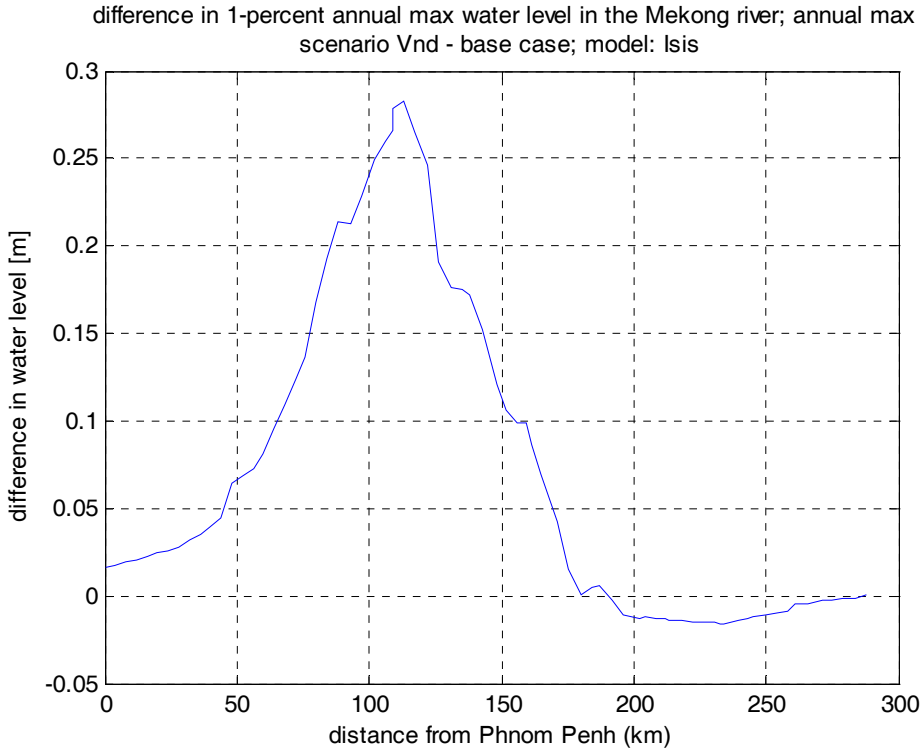

Figure 5.25 Increase in water level in the **Mekong** river downstream of Phnom Penh as a result of scenario **Vnd**.

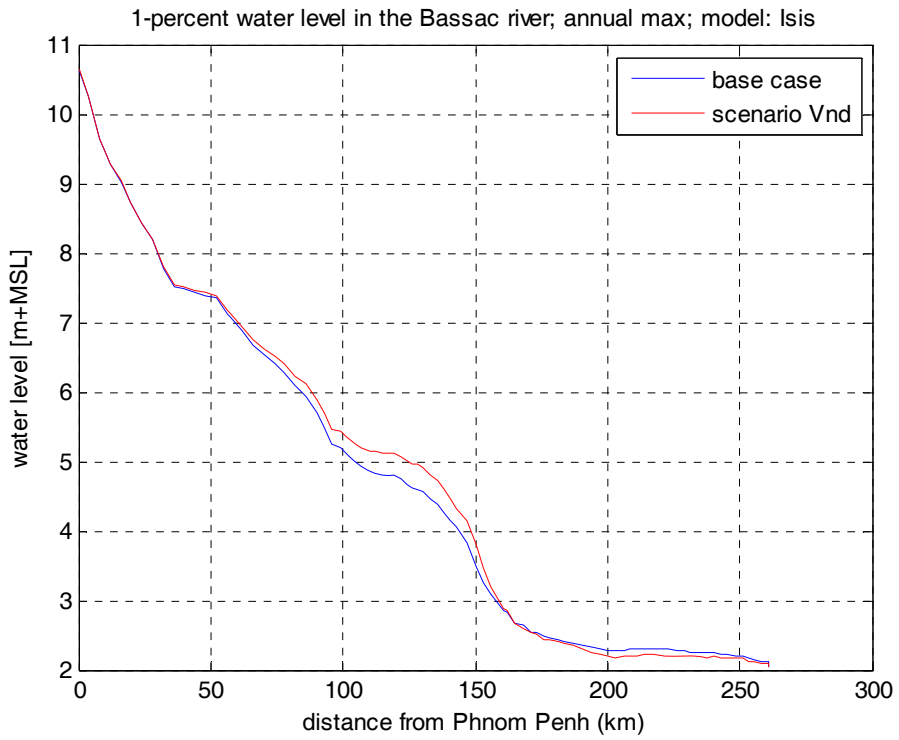

Figure 5.26 Water levels in the **Bassac** river downstream of Phnom Penh; comparison between the base case and scenario **Vnd**.

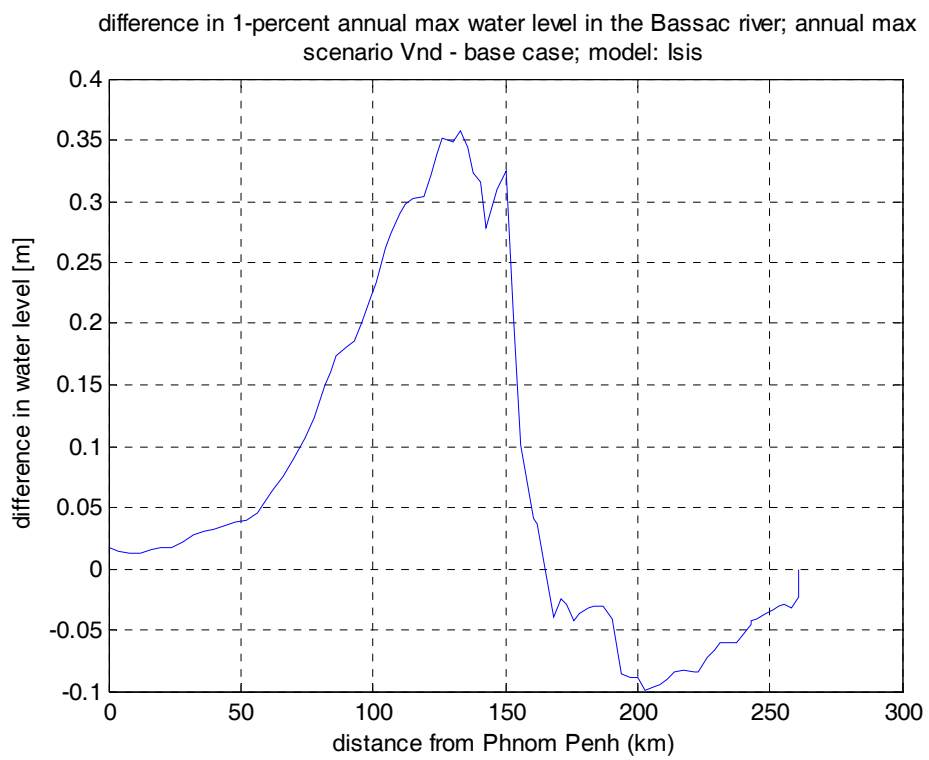

Figure 5.27 Increase in water level in the **Bassac** river downstream of Phnom Penh as a result of scenario **Vnd**.

5.4.6 Results for Scenario [5] – Cam0Vna

Figure 5.28 and Figure 5.29 show the differences in water levels between scenario Cam0Vna and base case for the 25 locations in Cambodia and 34 locations in Vietnam respectively. Again, for some locations the water levels increase as a result of the measures of scenario Cam0Vna, while for other locations the water levels decrease. Figure 5.30 - Figure 5.33 compare water levels with probabilities of exceedance of 1% in the Mekong and Bassac rivers for the base case and scenario Cam0Vna.

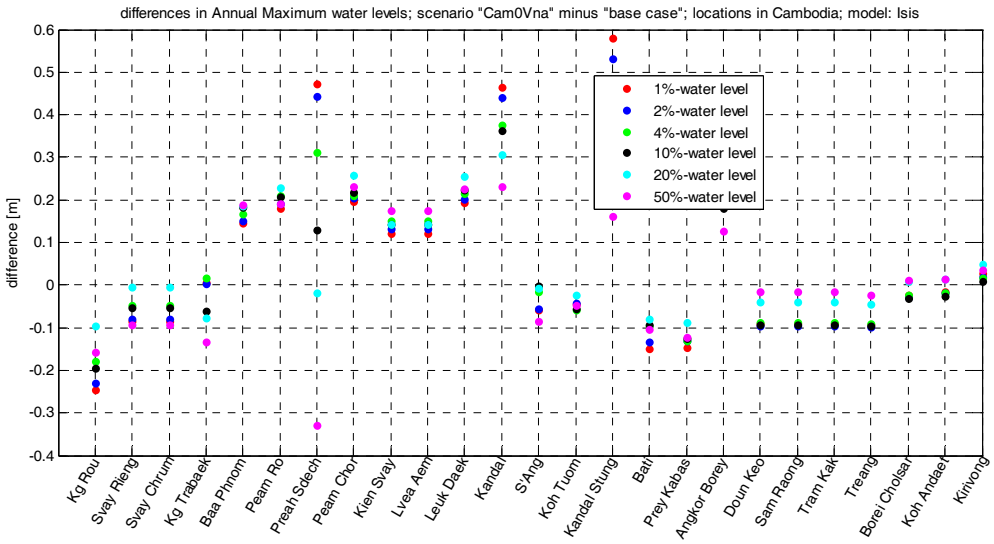

Figure 5.28 Change in the p-percent annual maximum water level (p=1, 2, 4, 10, 20 and 50) for 25 locations in **Cambodia**; comparison of scenario **Cam0Vna** with the base case. Positive values indicate an increase in water level.

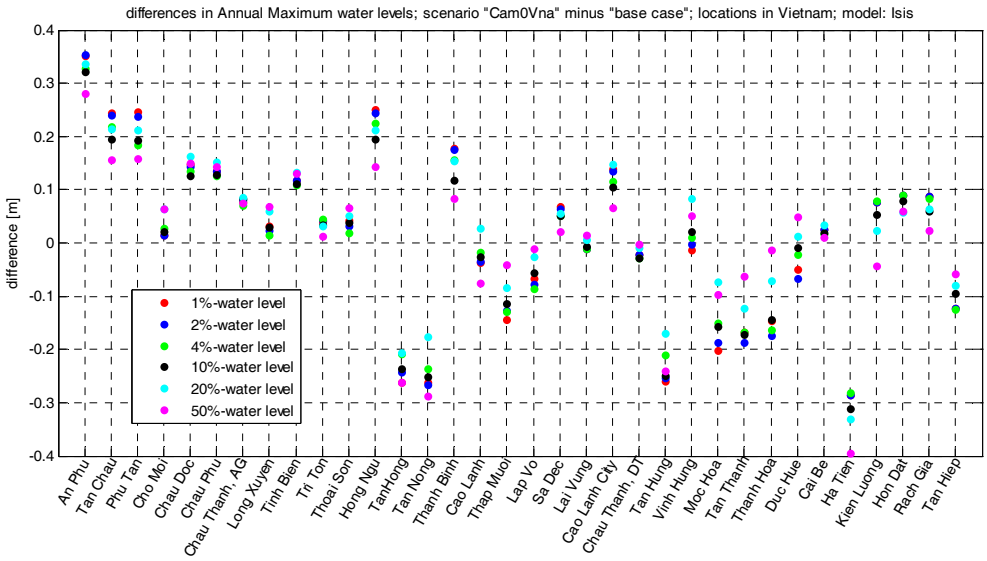

Figure 5.29 Change in the p-percent annual maximum water level (p=1, 2, 4, 10, 20 and 50) for 34 locations in **Vietnam**; comparison of scenario **Cam0Vna** with the base case. Positive values indicate an increase in water level.

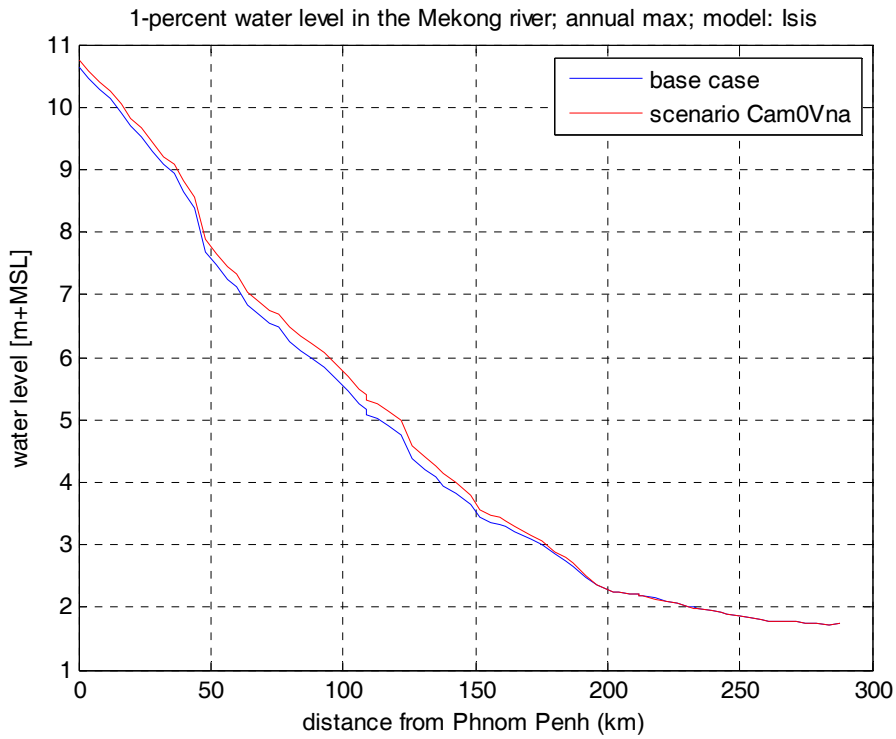

Figure 5.30 Water levels in the **Mekong** river downstream of Phnom Penh; comparison between the base case and scenario **Cam0Vna**.

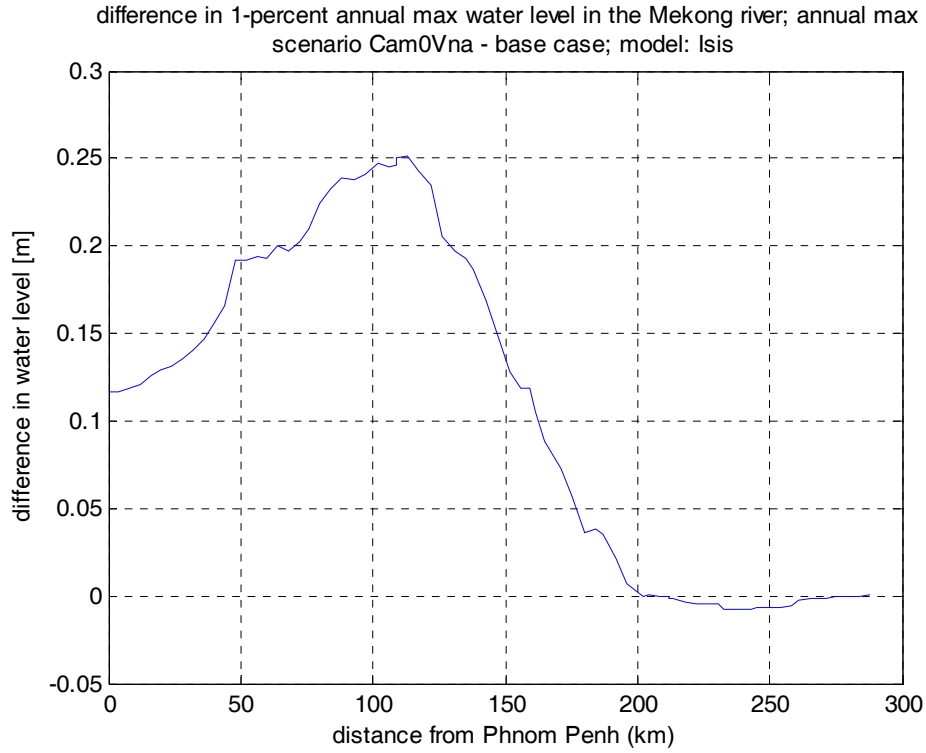

Figure 5.31 Increase in water level in the **Mekong** river downstream of Phnom Penh as a result of scenario **Cam0Vna**.

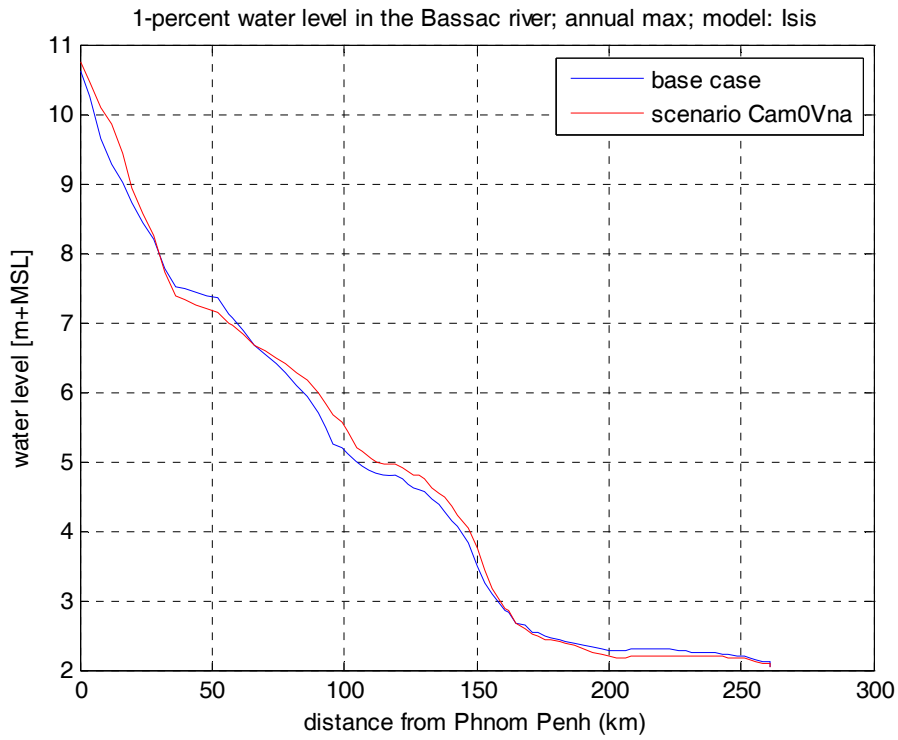

Figure 5.32 Water levels in the **Bassac** river downstream of Phnom Penh; comparison between the base case and scenario **Cam0Vna**.

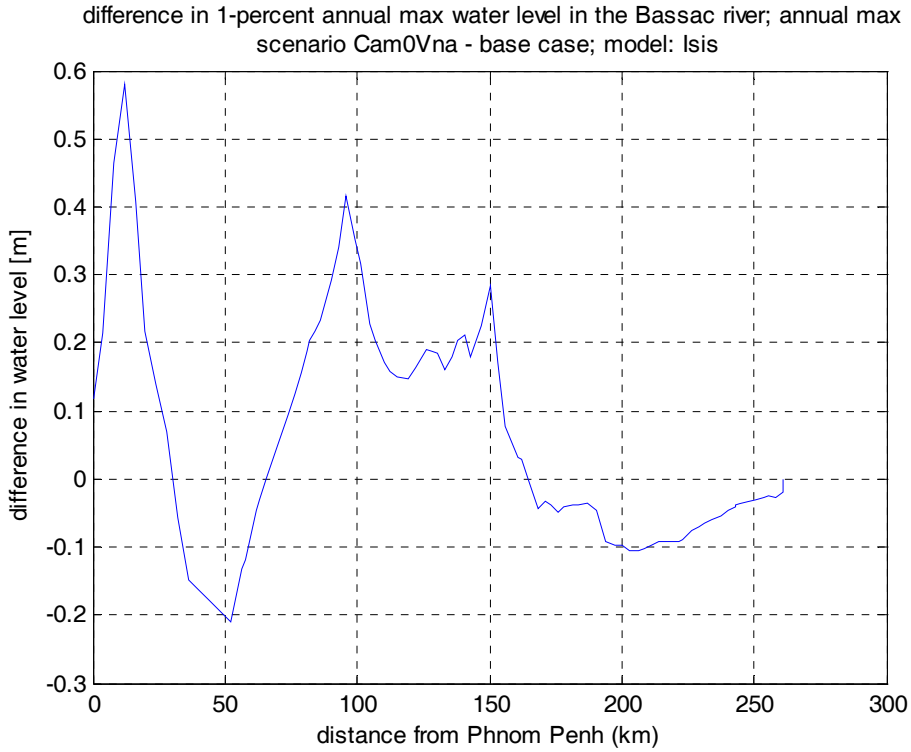

Figure 5.33 Increase in water level in the **Bassac** river downstream of Phnom Penh as a result of scenario **Cam0Vna**.

5.5 Scenario [6] – flood diversion to the Tonle Sap lake

In Cambodia the paddy is harvested before 1 August each year according to the crop calendar. In Vietnam the crop is harvested before the third week of August. When floods occur before the date of harvest it will create damage to the crop. Hence, if the floods can be limited till after the date of harvest up to the capacity of the Mekong and Bassac downstream of Phnom Penh, then benefits are generated for the farmers. In Scenario_4 this is achieved by diversion of flood water to the Tonle Sap for early flood control. Additional benefits of such option is generated for fish farming in the Lake as the Tonle Sap Lake level will be higher than normal. Furthermore, if the outflow from the Lake is controlled the water availability for the dry season increases, which provides options to reduce salinity problems in the delta.

The effectiveness of flow diversion to Tonle Sap from midway Kampong Cham-Phnom Penh to the Lake has been investigated for two variants:

1. a fully controlled diversion, and
2. an uncontrolled diversion.

For this a water balance model of the Mekong between Kampong Cham and Phnom Penh has been developed, including Tonle sap River and Lake and a diversion canal from the Mekong to the Lake, see Figure 5.34. In the controlled mode, the diversion is operated such that the flow downstream of Phnom Penh does not exceed the capacity of the rivers Mekong and Bassac, set to 30,000 m3/s. Limits are further set to the diversion capacity, and Tonle Sap River capacity (10,000 m3/s) and Tonle Sap Lake volume (85.86 BCM i.e. equivalent to a Lake level of 11.0 masl). The model is run for the 97 historical flood seasons, see Chapter 4.

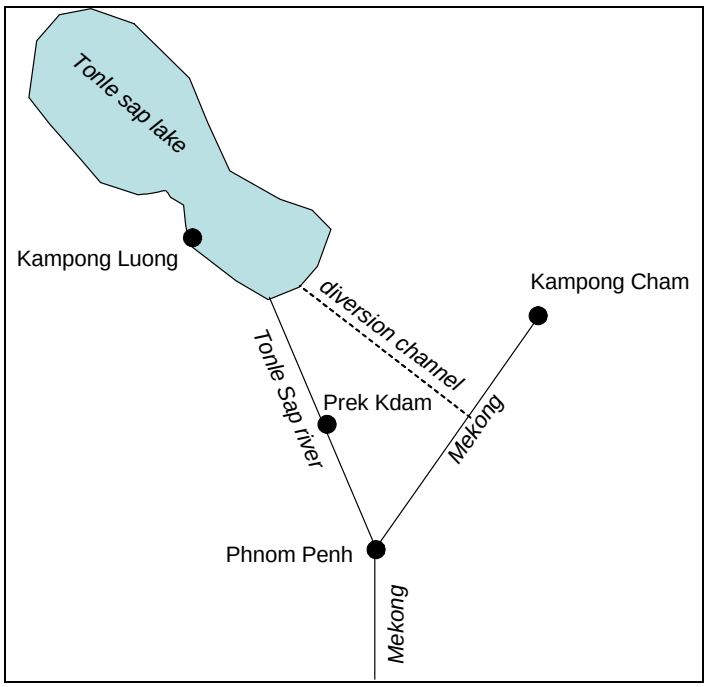

Figure 5.34 Structure of water balance model of Mekong and Tonle Sap

Controlled diversion

For the controlled diversion the effectiveness of the measure for different diversion capacities can be read from Figure 5.35.

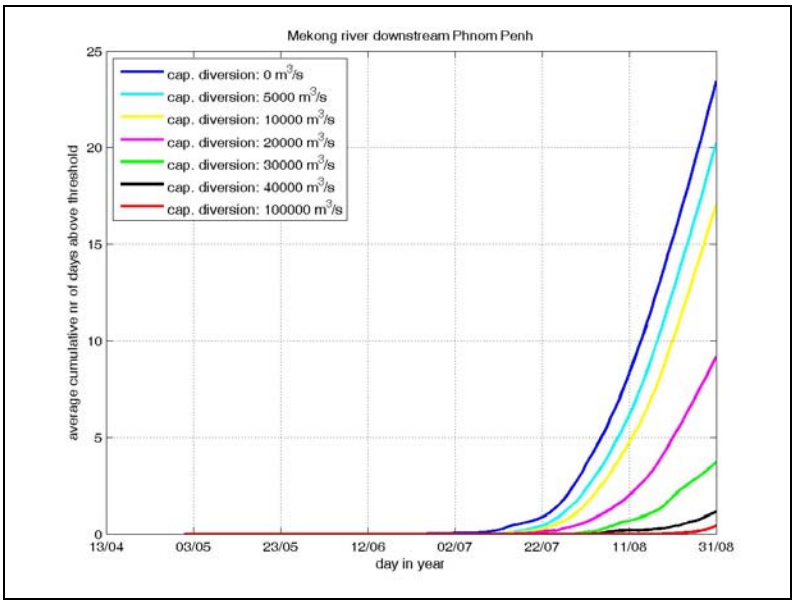

Figure 5.35 Average cumulative number of days (up to the date shown on the horizontal axis) in the simulated period 1910-2006 during which the flow downstream of Phnom Penh exceeded 30,000 m^3/s; depending on the available flow capacity of the diversion channel

The graph shows that under present conditions the number of days that flooding takes place downstream of Phnom Penh before 1 August is about 3 days on average each year. This would reduce to 1 day with a diversion canal with a capacity of 20,000 m^3/s. before the third week of August on average during 16 days flooding occurs, whereas with a diversion canal of the same capacity this would reduce to about 5. Figure 5.36 shows the mean wet surface area of the lake for different values of the flow capacity of the diversion channel. It shows the area increases with increasing capacity. Generally, an increase in the wet surface area has a positive effect on the fish population.

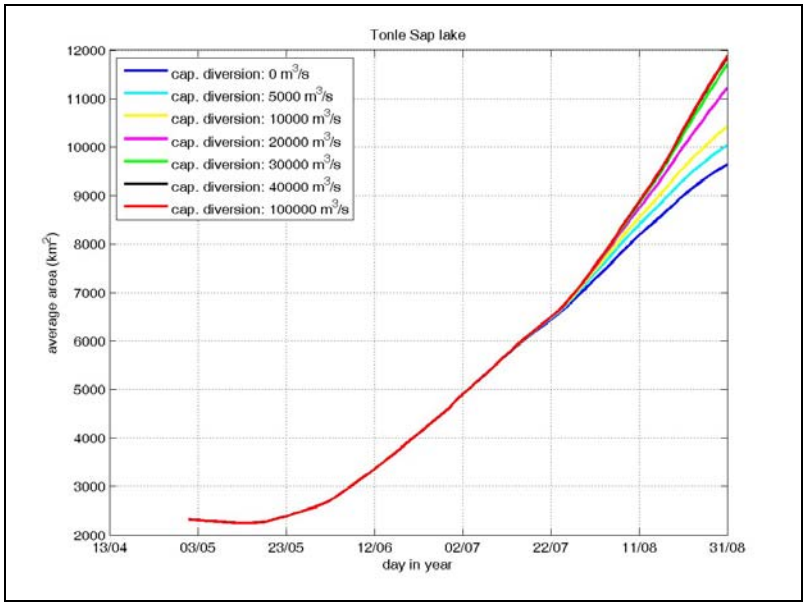

Figure 5.36 Mean wet surface area of the lake for different values of the flow capacity of the diversion.

Uncontrolled diversion

For the uncontrolled diversion a 2,500 m wide diversion canal is assumed with a weir at the off-take having a fixed level of 8.0 masl. The effectiveness of this measure seems to be limited as is observed from Figure 5.37 at first glance. However, this is mainly due to the fact that this option cannot control the flow downstream of Phnom Penh not to exceed exactly 30,000 m^3/s. The flood volume, though, will reduce substantially.

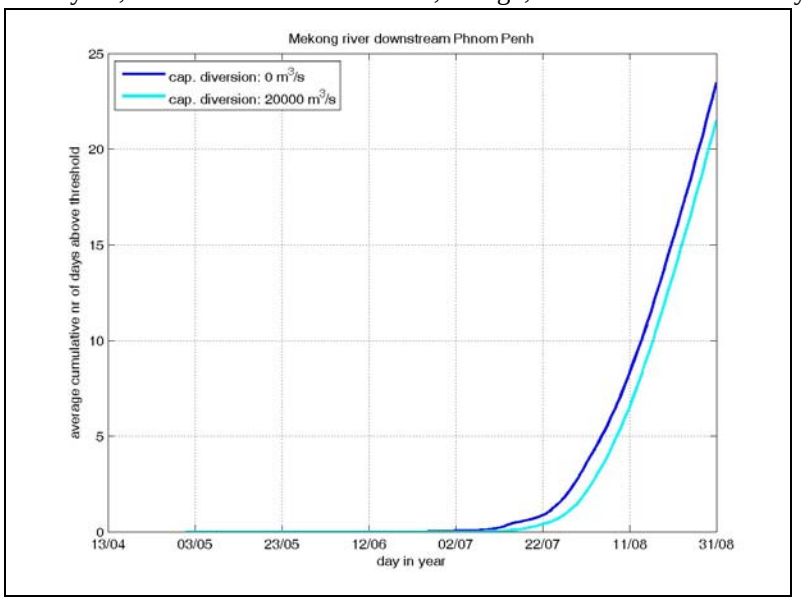

Figure 5.37 Average cumulative number of days (up to the date shown on the horizontal axis) in the simulated period 1910-2006 during which the flow downstream of Phnom Penh exceeded 30,000 m^3/s; depending on the available flow capacity of the diversion channel.

So the benefit of the uncontrolled channel can be found in the volume of water that fills the flood plain. This volume will be reduced each year the water flows into the diversion channel. For each year in the simulation period 1910-2006 the volume above the threshold of

30,000 m^3/s was derived. Figure 5.38 and Figure 5.39 show the frequency distributions of these volumes as derived on August 1st and August 21st each year. It shows that especially at August 1 there is a large percentage-wise reduction of flood volume, indicating that the diversion channel prevents significant areas of farmland from flooding before the end of the growing season.

The uncontrolled diversion has also been simulated with the hydraulic model for the same flood seasons as selected for the Scenarios_1 to 3. An unregulated diversion canal diverting Mekong water into the Lake from an off-take at Khchau village was implemented. It turned out the maximum flood water levels are only slightly reduced by this Scenario, as its function has finished before the peak passes. The reduction on the early flood levels is somewhat larger but still very limited. By blocking the early return flow from the Tonle Sap the diversion channel option can be made more effective.

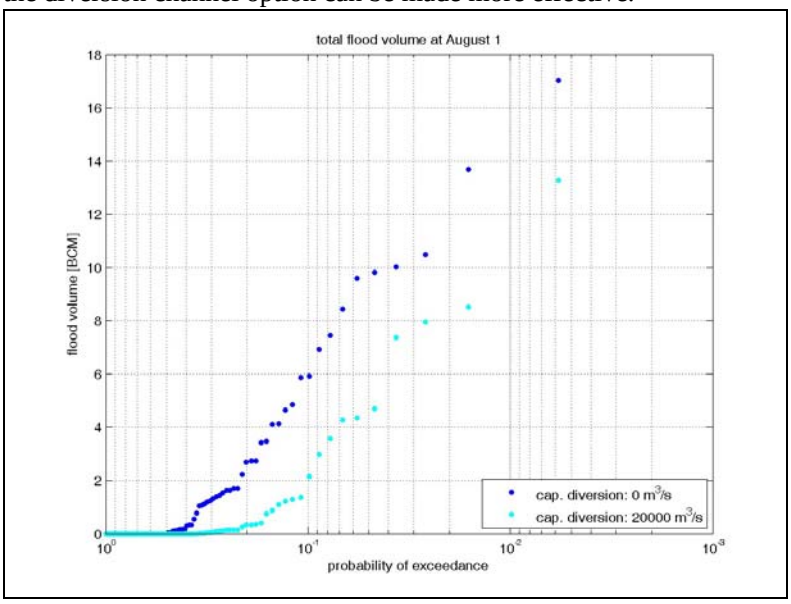

Figure 5.38 Frequency distribution of the total volume above a threshold of 30,000 m^3/s in the Mekong downstream of Phnom Penh until August 1, depending on the available flow capacity of the diversion channel.

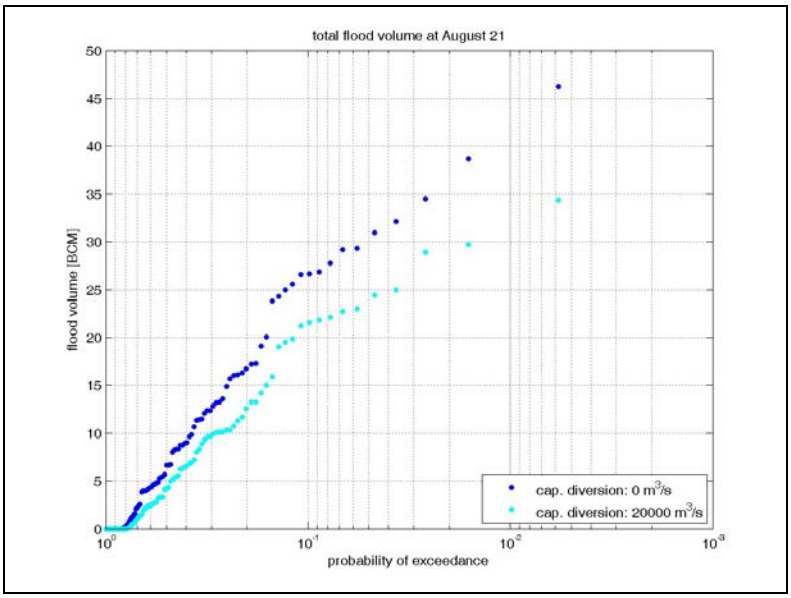

Figure 5.39 Frequency distribution of the total volume above a threshold of 30,000 m^3/s in the Mekong downstream of Phnom Penh until August 21, depending on the available flow capacity of the diversion channel.

5.6 Sea level rise

The following section is based on simulations with ISIS before the major improvements of August - September 2009 were carried out. In fact, the analysis of impact of see level rise should be done again. However, since impacts are essentially in the coastal zone of the delta, we see no need to re-simulate the case.

Due to climate change (melting of ice and particularly thermal expansion of water) the levels at sea at the mouth of the Mekong will rise in the next century with some 0.25 to 0.50 m (IPCC, 2007). This will affect the flood risk in the Mekong Delta. To get an impression of the effect of sea level rise on the water levels in the delta (size and extent) the Mekong Delta hydraulic model was run for two cases:

1. the Base Case: the year 2000 flood conditions using the observed sea level boundary and current hydraulic infrastructure
2. the Sea Level Rise Case; the year 2000 flood conditions using a 1 m higher sea level as boundary and the current hydraulic infrastructure.

The results of the computations are presented in Figure 5.40 to Figure 5.43 and Table 5.2.

Table 5.2 Effect of 1 m sea level rise on maximum water levels along Bassac and Mekong

Location	Distance, m	Maximum stage with	Maximum stage without	Diff.	Location	Distance, m	Maximum stage with	Maximum stage without	Diff.
Bassac					**Mekong**				
Phnom Penh	0.0	10.12	10.09	0.03	Phnom Penh	0.0	10.12	10.09	0.03
Koh Khel	48,000.0	6.99	6.95	0.04	Neak Luong	64,000.0	6.88	6.83	0.04
Chau Doc	119,003.1	4.82	4.66	0.15	Tan Chau	106,000.0	5.25	5.12	0.12
Long Xuyen	168,203.1	3.12	2.37	0.76	Cao Lanh	156,000.0	3.67	3.26	0.40
Can Tho	217,203.1	2.94	2.07	0.88	My Thuan	202,137.5	2.97	2.13	0.84
Dai Ngai	258,203.1	2.97	2.09	0.88	My Tho	243,297.5	2.75	1.86	0.89
					Ha Binh	265,969.0	2.72	1.76	0.96

Though exact linear interpolation on the differences for other seas level rises by multiplying the table values with the expected rise in meters will not be fully correct, as a first estimate it will be sufficient. Effects reduce on Bassac rapidly upstream of Long Xuyen. Along the Mekong the effect reduced strongly between My Thuan and Than Chau. The effect of the sea level rise has reduced to 12 to 15% at the Cambodian-Vietnamese border.

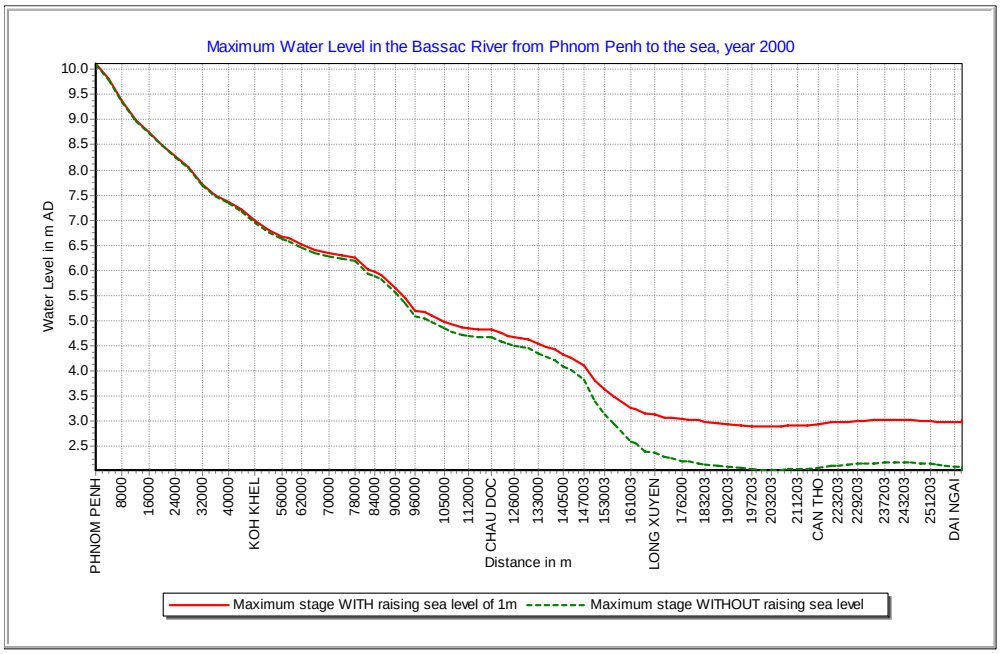

Figure 5.40 Effect of 1 m sea level rise on the maximum water level in Bassac, conditions of year 2000

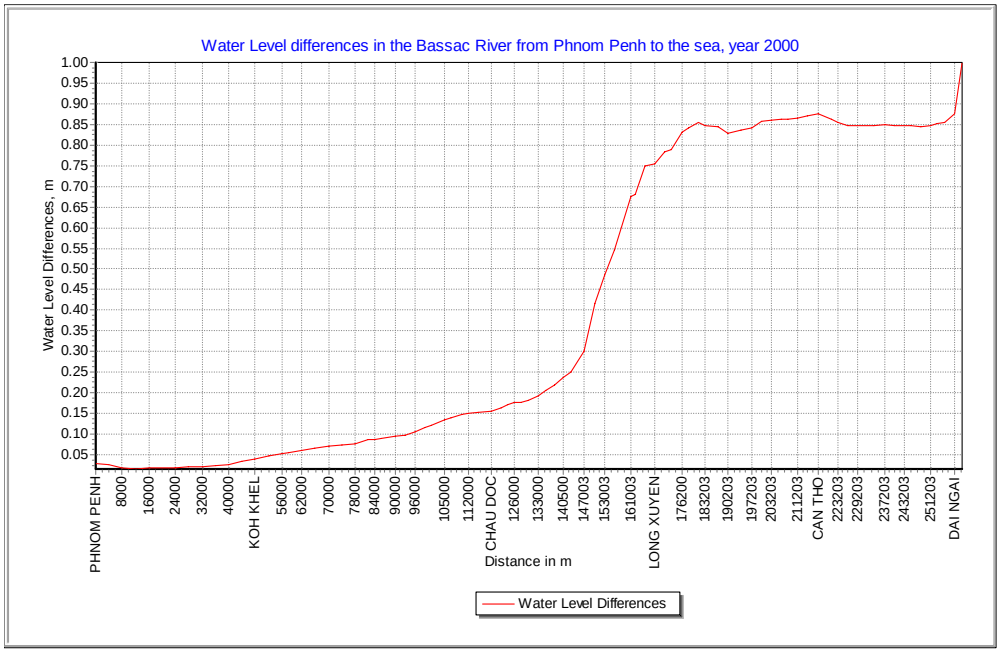

Figure 5.41 Net effect of 1 m sea level rise on the maximum water levels in Bassac, conditions of year 2000

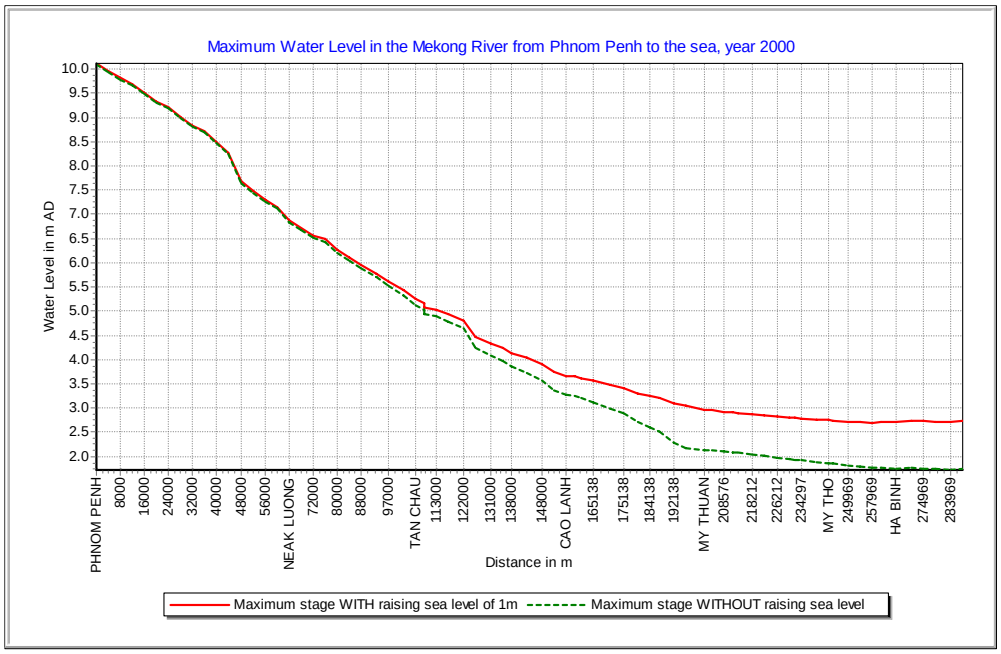

Figure 5.42 Effect of 1 m sea level rise on the maximum water level in Mekong, conditions of year 2000

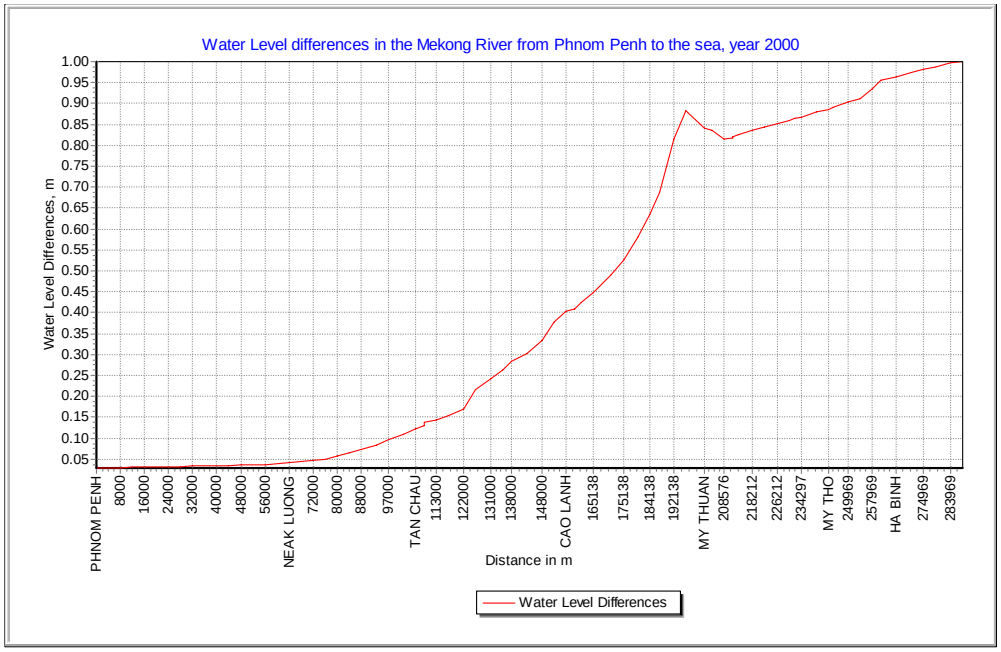

Figure 5.43 Net effect of 1 m sea level rise on the maximum water level in Mekong, conditions of year 2000

6 Conclusions and recommendations

6.1 Conclusions

Flood hazard assessment procedures

- Flood hazard in the Mekong delta up to return period of 100 years is determined from frequency analysis of 97 years of flood hydrographs derived with the Mekong Delta hydraulic model for the historical flow from 1910 to 2006.
- The Mekong Delta hydraulic model needs recalibration and refinement of the schematization of the Focal Areas in Cambodia. At present the model output is acceptable for demonstration purposes but unsuitable for planning or design.
- The inflow series to the Mekong delta can at present best be taken from the discharge series of the Mekong at Stung Treng. This series was considered to be more reliable and also available for a longer period. The use of the series of Kratie is not recommended because it is unreliable. The flow at Stung Treng is, apart from a time shift of one day, approximately equal to the flow at Kratie.
- The discharge series both at Stung Treng and Kratie contain a discontinuity caused by change in use of discharge measuring equipment. For a particular water level the current meter method leads to higher discharges then an ADCP.
- The combined flow of the tributaries of the to Tonle Sap Lake (Tonle Sap river not included) is correlated with the flow of the Mekong river at stung Treng. To correctly generate monthly inflow series the serial correlation with the flow in the previous month and the cross-correlation with the inflow to the delta in the same month should be taken into account.
- The seasonal rainfall in the Mekong Delta shows no significant correlation with the inflow to Tonle Sap nor the Mekong flow at Kratie.
- The hydraulic model of the Mekong Delta uses in its simulations the observed water levels in the Gulf of Thailand and in the South China Sea as boundary condition. This series slightly underestimates the average conditions along the coast (0.07 m at Tra Vinh).
- A realistic 97 year long set of boundary conditions has been created for the Mekong Delta model.

Development scenarios

- The various scenarios of flood control measures (Cam0, Vna, Vnd and Cam0Vna) result in reduced water level at several locations, but at the same time cause an increase at other locations. Analysis of expected damage (see for example Volume 2C and Volume 3A) will show whether these measures have a net benefit when all 59 district are taken taken into account.
- The scenarios of development in Vietnam (Vna and Vnd) cause rising water levels in all 25 locations in Cambodia.
- The regime of the Mekong is about 1 month ahead of the Tonle Sap local inflow regime, which provides opportunities to use the lake for storage of early Mekong floodwater to reduce damage to crop.

- Diversion of flow to the Tonle Sap may have mutual benefits, including early flood volume reduction, which reduces damage to unharvested crop, extended surface area of Tonle Sap, which benefits fish farming and larger volume of water stored in Tonle Sap, which when the outflow is controlled, can be used to reduce the salt intrusion in the delta.
- Controlled diversion of Mekong flood water to Tonle Sap Lake is an effective tool to reduce early floods downstream of Phnom Penh up to a discharge of 30,000 m^3/s and leads to larger volumes of water stored in Tonle Sap Lake.
- Uncontrolled diversion of Mekong flood water to Tonle Sap Lake hardly reduces the exceedance frequency of a discharge of 30,000 m^3/s downstream of Phnom Penh up till 31 August. Its effect on reducing early flood volumes is substantial.
- Despite the latter, the effect of uncontrolled flooding on reduction of early flood levels in the Focal Areas is only 1 to 2 dm and proved to be far less effective then local flood protection measures.

6.2 Recommendations

Based on the analyses made in the frame of flood hazard assessment for the Mekong delta it is strongly recommended to improve on the computational tools available at the MRC. The recalibration of the Mekong Delta hydraulic model is to be undertaken with priority including an extension of the computational network in the Focal Areas in Cambodia. Prior to the recalibration, during the 2008 flood season concurrent current meter and ADCP discharge measurements have to be made at Kratie to resolve in-homogeneities in the inflow series of the Mekong Delta.

The effects of the development alternatives are recommended to be repeated with the hydraulic model using the updated schematisation of the Focal Areas in Cambodia. Then also controlled diversion of flood water to the Tonle Sap, including an outflow control structure in the Tonle Sap River, to maximise the benefits of extra storage of water within the basin is recommended to be evaluated.

7 Literature

IPCC (2007)
Climate Change 2007.
IPCC Fourth Assessment Report

Royal Haskoning, Delft Hydraulics and IHE (2008)
Character and Nature of Flooding in the Lower Mekong Basin.
Volume 2: Appendix 1 of Inception Report of the Flood Management and Mitigation Program, Component 2: Structural Measures and Flood Proofing

Attachment 1.1: Flood Hazard map at p=1%, Base case, Year Maximum

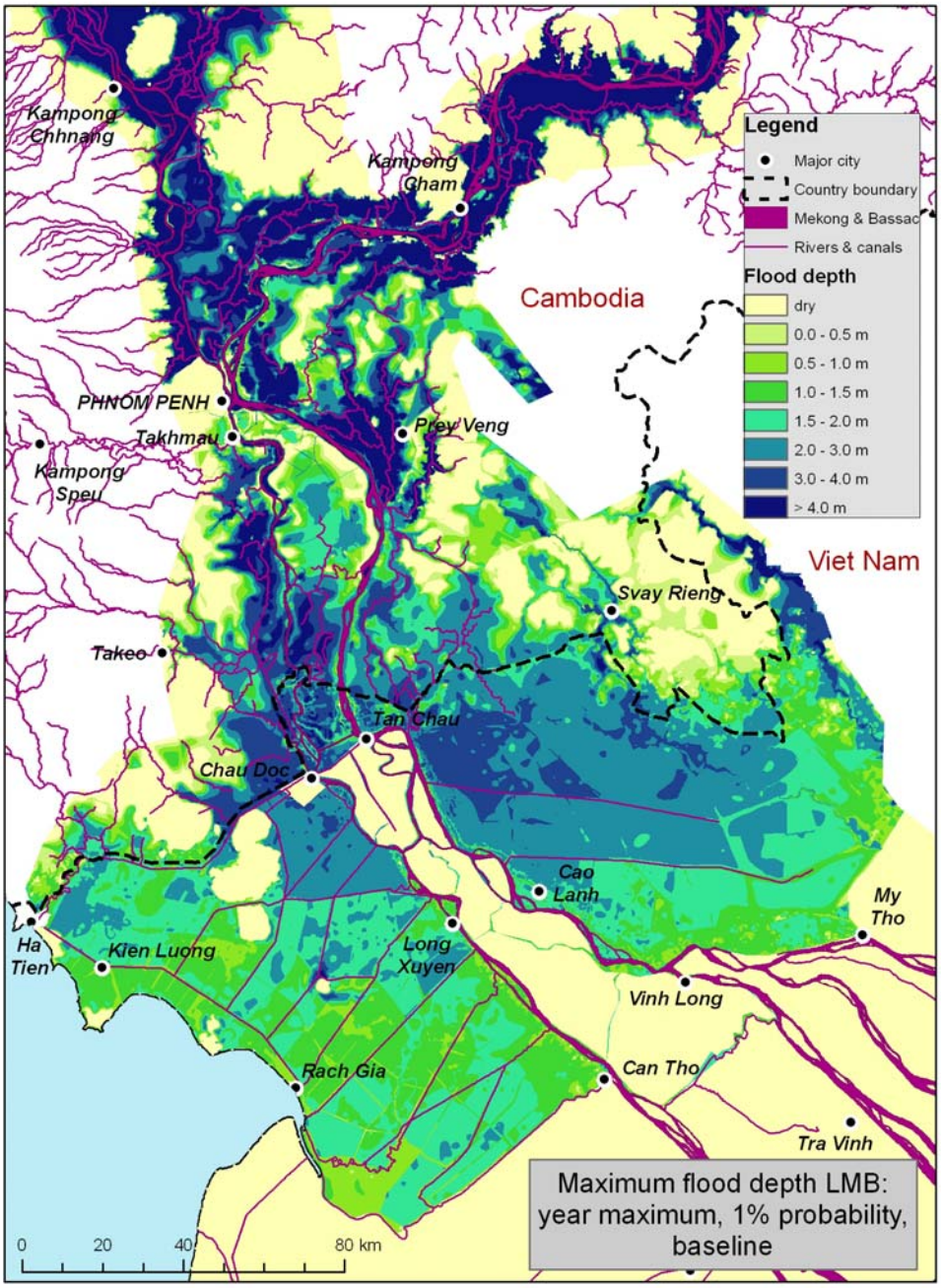

Attachment 1.2: Flood Hazard map at p=4%, Base case, Year Maximum

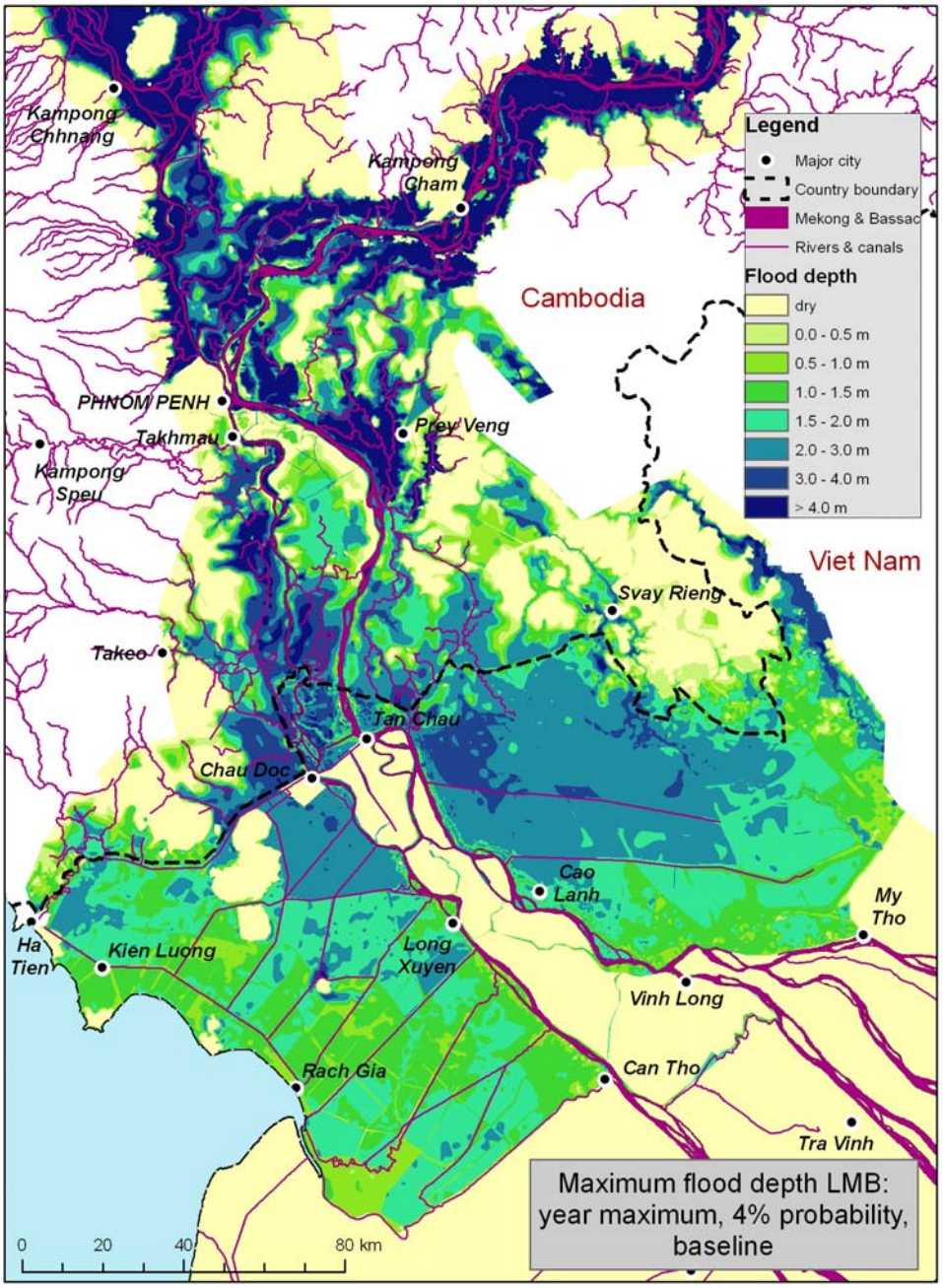

Attachment 1.3: Flood Hazard map at p=10%, Base case, Year Maximum

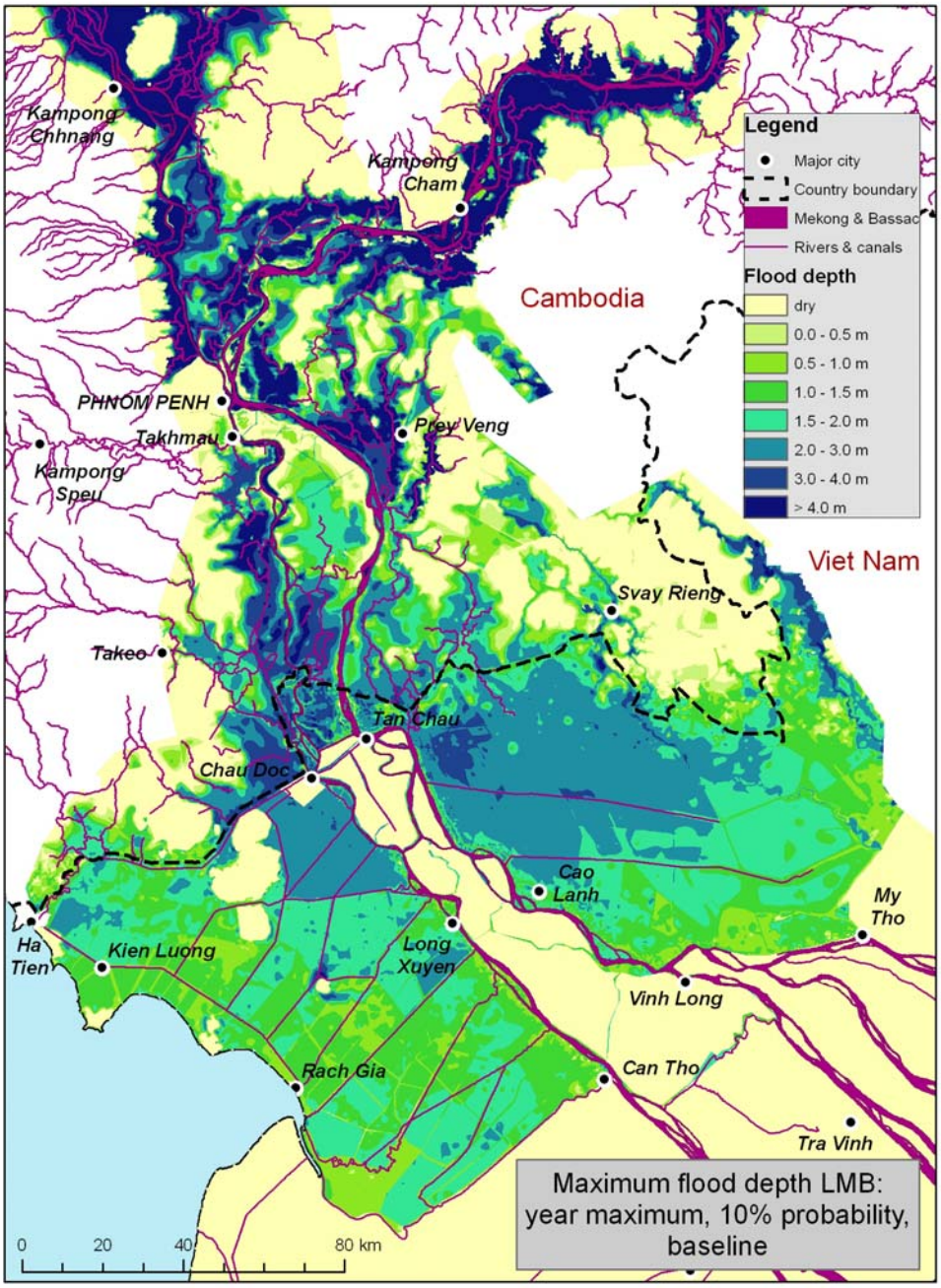

Attachment 1.4: Flood Hazard map at p=20%, Base case, Year Maximum

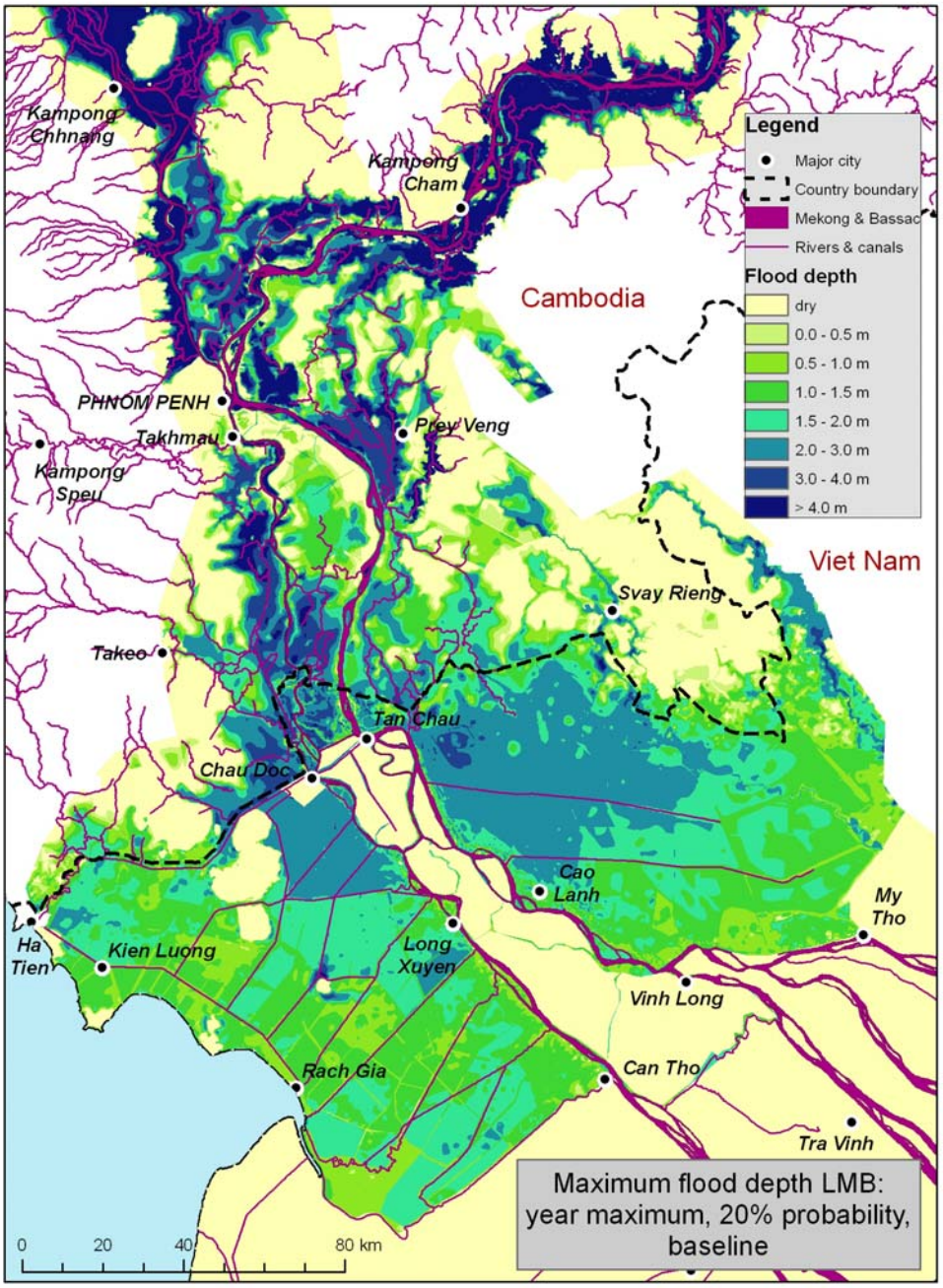

Attachment 1.5: Flood Hazard map at p=50%, Year Maximum

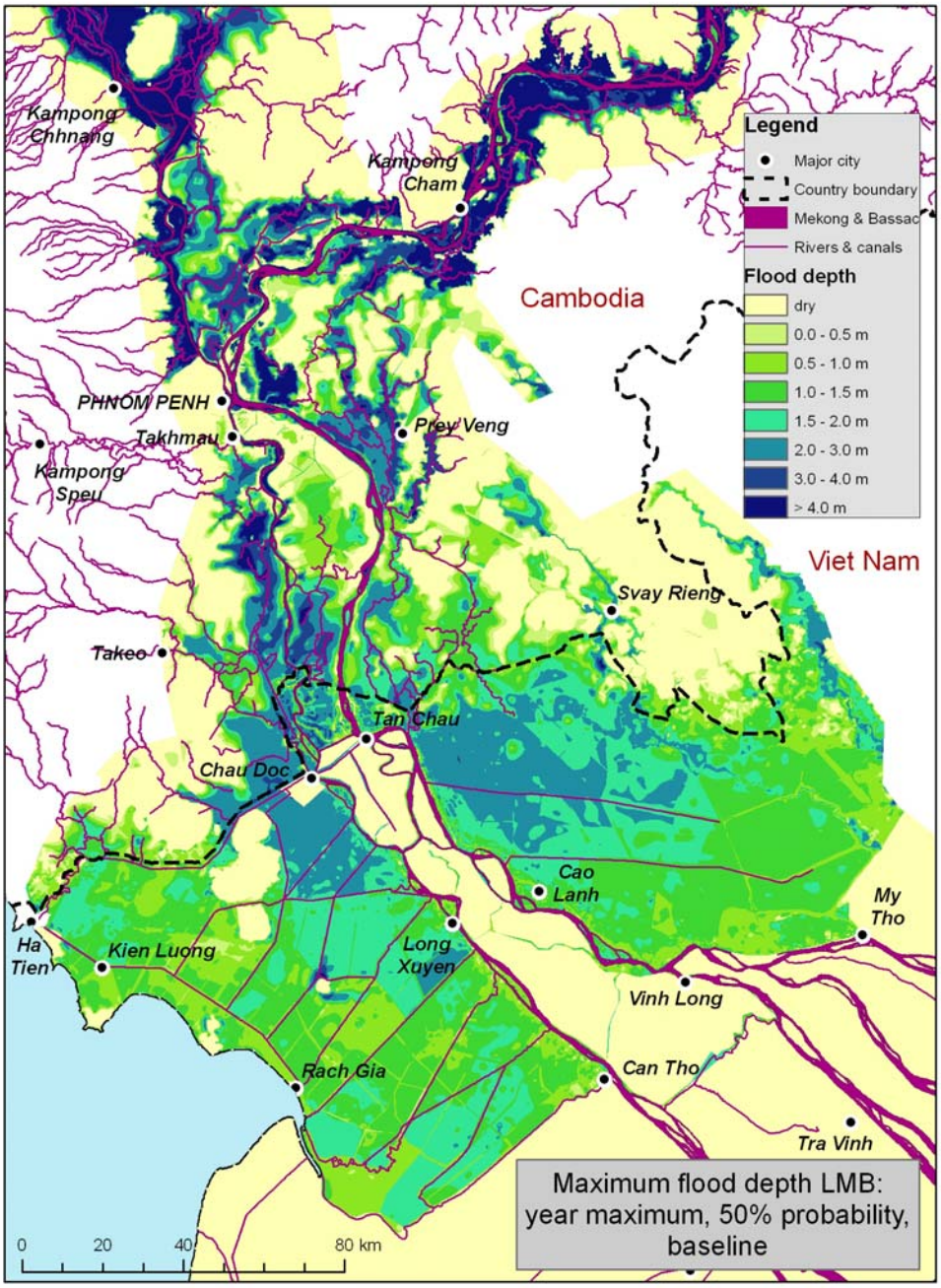

Attachment 1.6: Flood Hazard map at p=1%, Base case, Before 1st of August

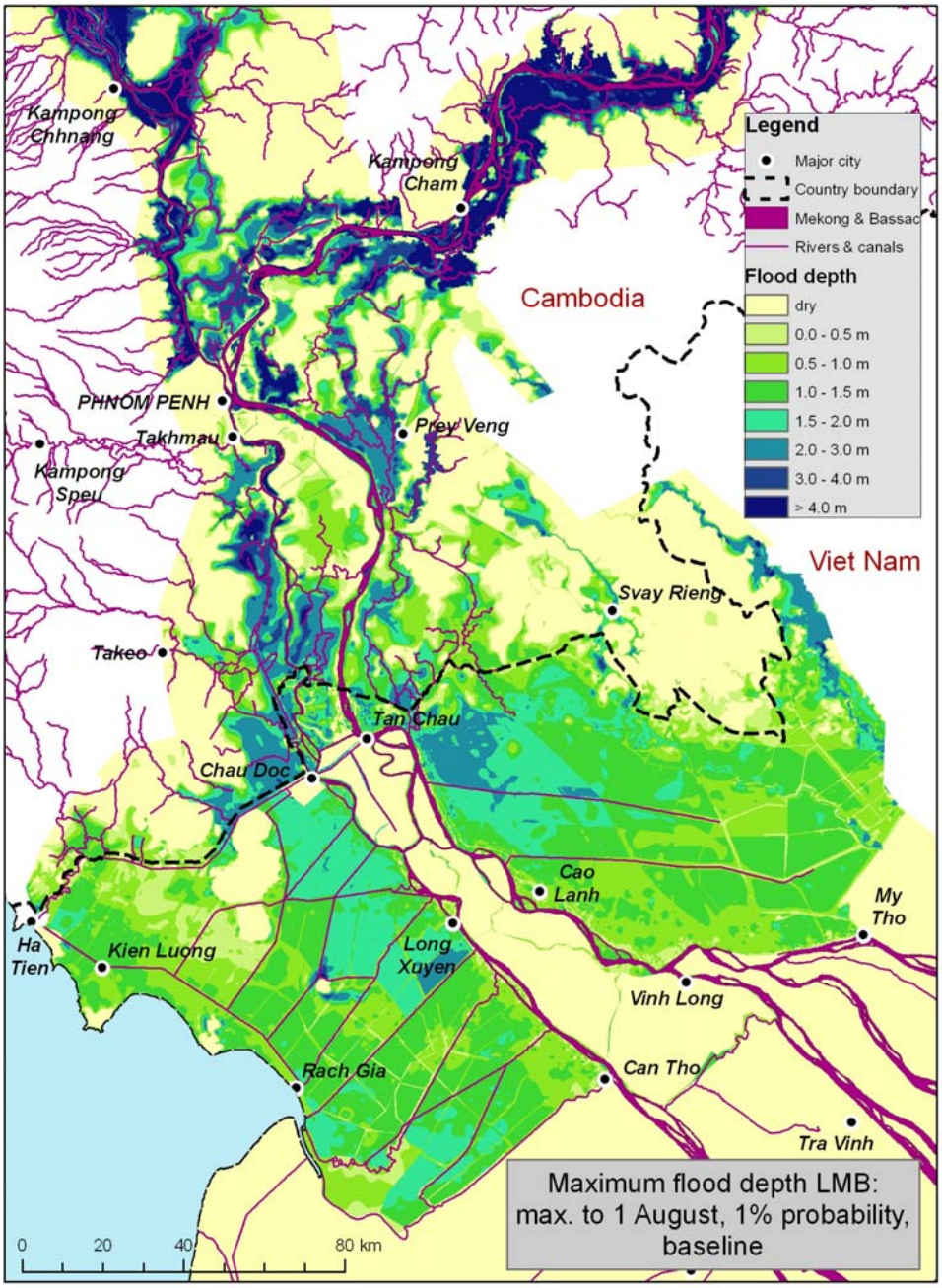

Attachment 1.7: Flood Hazard map at p=4%, Base case, Before 1st of August

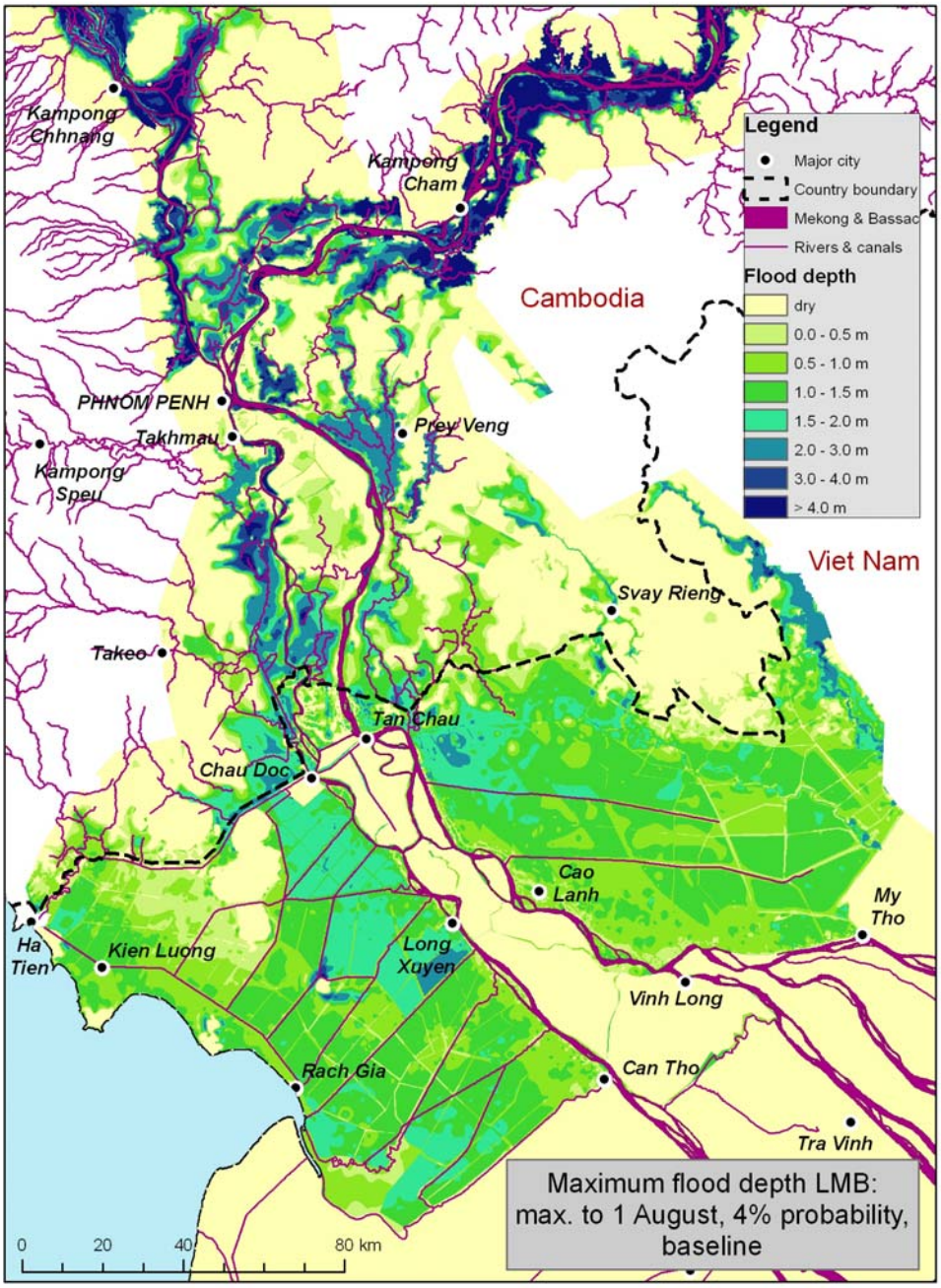

Attachment 1.8: Flood Hazard map at p=10%, Base case, Before 1st of August

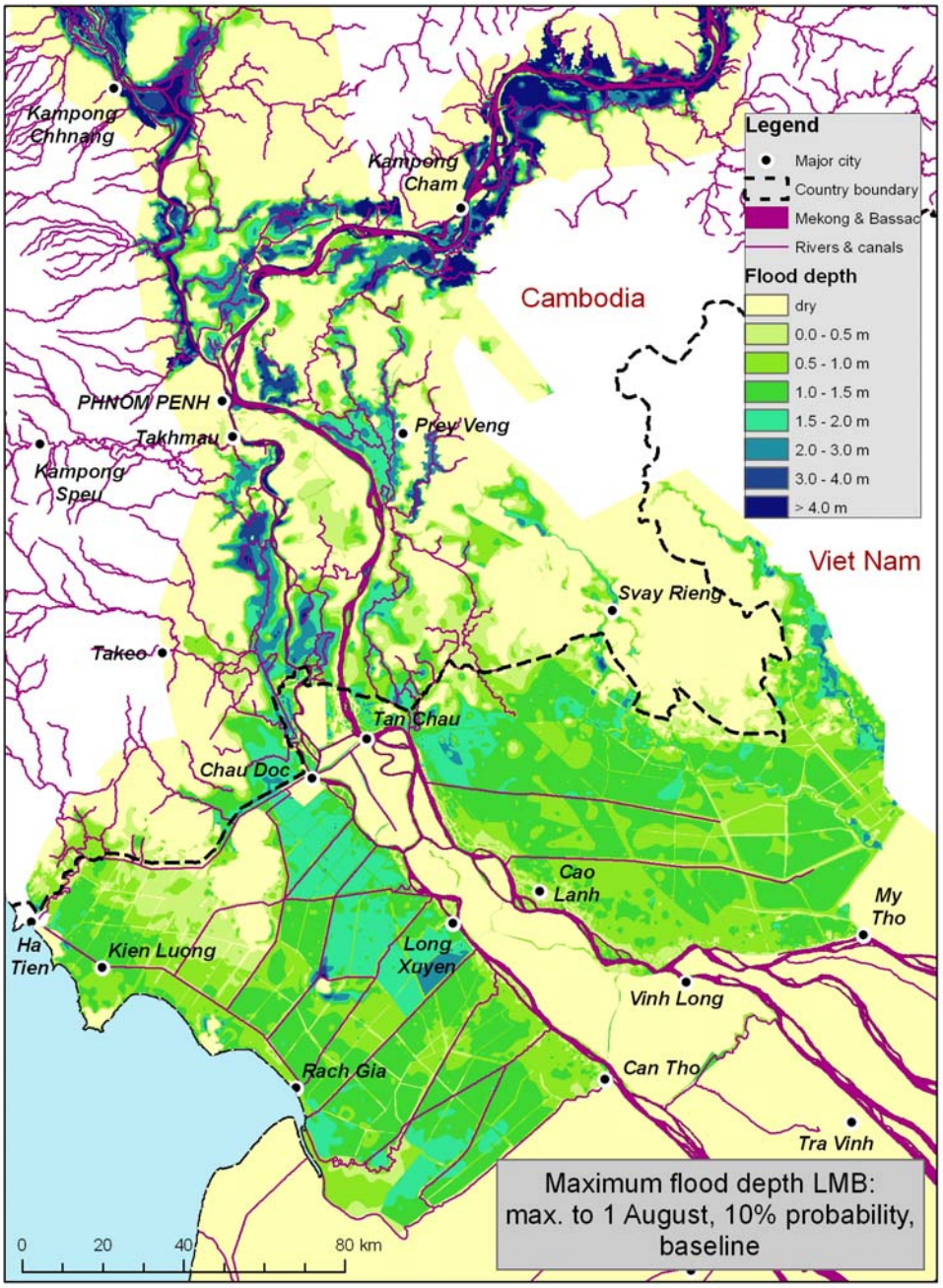

Attachment 1.9: Flood Hazard map at p=20%, Base case, Before 1st of August

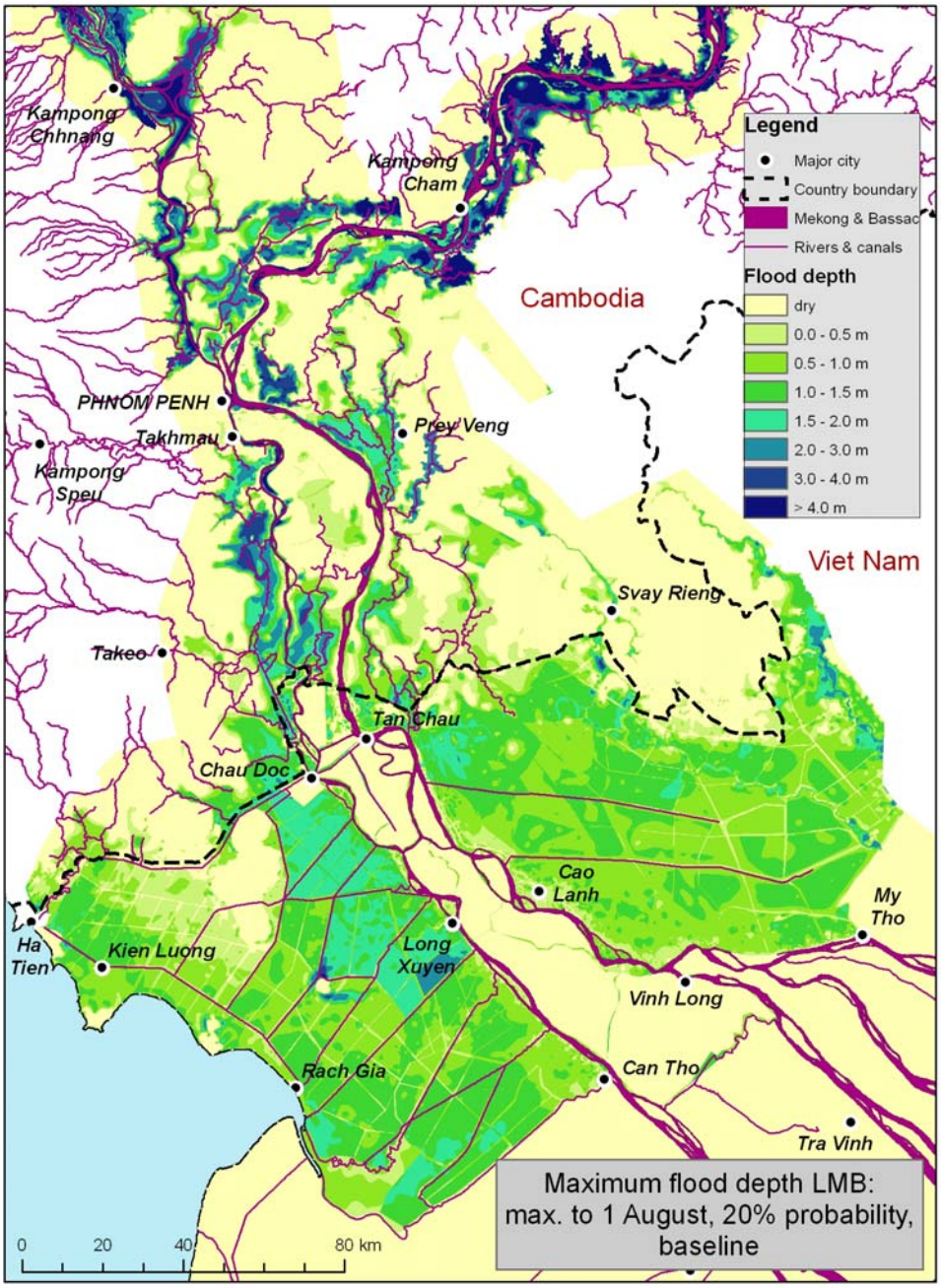
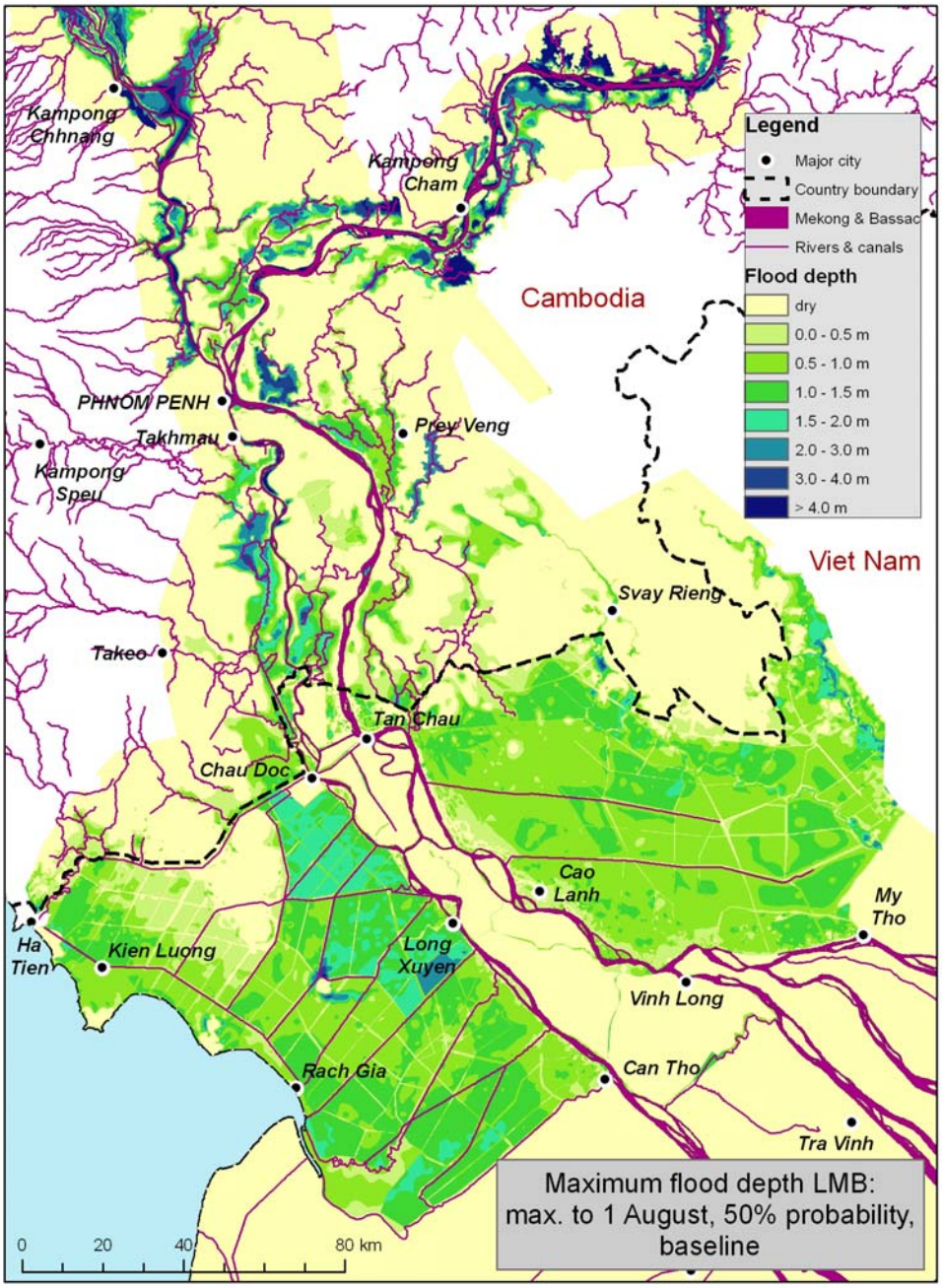
Attachment 1.10: Flood Hazard map at p=50%, Base case, Before 1st of August